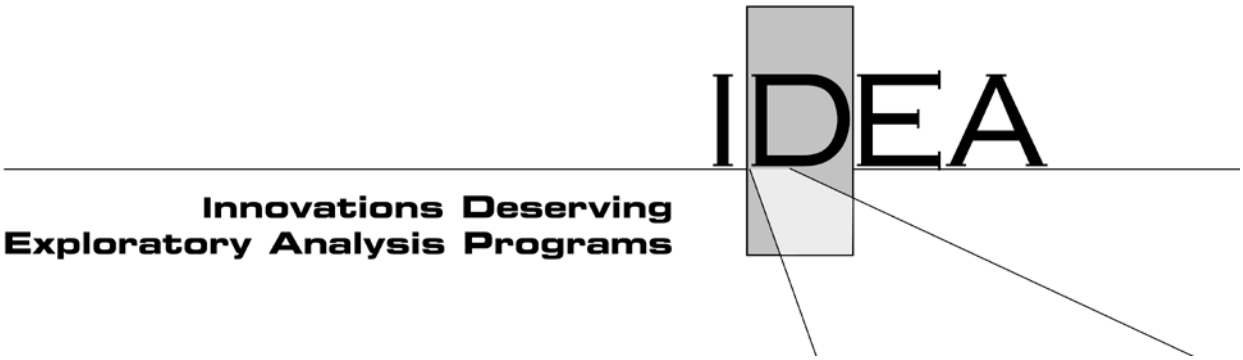

NCHRP IDEA Program

Development of an Asphalt Pavement Raveling Detection Algorithm Using Emerging 3D Laser Technology and Macrotexture Analysis

Final Report for
NCHRP IDEA Project 163

Prepared by:
Yichang (James) Tsai, Zhaohua Wang
Georgia Institute of Technology

December 2015

TRB TRANSPORTATION RESEARCH BOARD
The National Academies of
SCIENCES · ENGINEERING · MEDICINE

Innovations Deserving Exploratory Analysis (IDEA) Programs Managed by the Transportation Research Board

This IDEA project was funded by the NCHRP IDEA Program.

The TRB currently manages the following three IDEA programs:

- The NCHRP IDEA Program, which focuses on advances in the design, construction, and maintenance of highway systems, is funded by American Association of State Highway and Transportation Officials (AASHTO) as part of the National Cooperative Highway Research Program (NCHRP).
- The Safety IDEA Program currently focuses on innovative approaches for improving railroad safety or performance. The program is currently funded by the Federal Railroad Administration (FRA). The program was previously jointly funded by the Federal Motor Carrier Safety Administration (FMCSA) and the FRA.
- The Transit IDEA Program, which supports development and testing of innovative concepts and methods for advancing transit practice, is funded by the Federal Transit Administration (FTA) as part of the Transit Cooperative Research Program (TCRP).

Management of the three IDEA programs is coordinated to promote the development and testing of innovative concepts, methods, and technologies.

For information on the IDEA programs, check the IDEA website (www.trb.org/idea). For questions, contact the IDEA programs office by telephone at (202) 334-3310.

IDEA Programs
Transportation Research Board
500 Fifth Street, NW
Washington, DC 20001

Development of an Asphalt Pavement Raveling Detection Algorithm Using Emerging 3D Laser Technology and Macrotexture Analysis

IDEA Program Final Report

Contract Number: NCHRP-163

Prepared for the IDEA Program
Transportation Research Board
The National Academies

Yichang (James) Tsai, Ph.D., P.E.

Zhaohua Wang, Ph.D., P.E.

Georgia Institute of Technology

Submittal Date: December 2015

ACKNOWLEDGMENTS

The work described in this report was supported by the National Academy of Sciences, National Cooperative Highway Research Program (NCHRP) Innovations Deserving Exploratory Analysis (IDEA) program. We would like to thank the Georgia Department of Transportation (GDOT); the Florida Department of Transportation (FDOT); the North Carolina Department of Transportation (NCDOT); the South Carolina Department of Transportation (SCDOT); the Kansas Department of Transportation (KDOT); the Department of Public Works, Nashville, Tennessee; and Fugro Roadware Inc., for their valuable inputs. We would like to thank Mr. Timothy Dale Brantley, Ms. Ernay Robinson, Mr. Eric Pitts (retired), and Mr. Thomas Mims from GDOT for their significant involvement in selecting test sections and collecting ground truth data. We would also like to thank the members of the Georgia Tech research team, Mr. Hadrien Glaude, Mr. Bruno Pop-Stefanov, Mr. Jinqi Fang, Mr. Yipu Zhao, and Dr. Chengbo Ai, for their diligent work. And, we thank Dr. Inam Jawed for his assistance in managing this project.

TABLE OF CONTENTS

EXECUTIVE SUMMARY

Raveling is one of the most common asphalt pavement distresses that occur on U.S. highway pavements. Raveling will increase pavement roughness, which results in poor ride quality and road and tire noise. Besides safety concerns, such as loose stones that may break windshield glass and can cause hydroplaning, raveling will also shorten pavement longevity. Thus, a raveling condition survey is required for highway agencies to determine the severity levels, the extents, and the locations of raveling so the preservation or rehabilitation treatments can be appropriately applied. However, the traditional raveling survey method, including determination of the raveling severity level (e.g., Low, Moderate, or High; or Severity Level 1, 2, or 3), extent, and location is a visual inspection that is time consuming, subjective, and hazardous to highway workers. Thus, there is an urgent need for developing an automatic survey method. Although some algorithms have been developed to detect and classify raveling, they are still at the very early research stage and the outcomes were often not acceptable. In addition, they have not been thoroughly validated using large-scale, real-world data. Therefore, it has been difficult for transportation agencies to implement any of such algorithms. To address the problems in existing raveling detection and classification methods, the objective of this study is to develop successful and effective raveling detection, classification, and measurement algorithms using three-dimensional (3D) pavement data and macro-texture analysis, and to comprehensively validate these methods using large-scale, real-world data. The developed algorithms, using 3D pavement data and the accompanying two-dimensional (2D) intensity data, include the following five components:

- Data pre-processing to remove data outliers, detect pavement markings and edge drop-off, and extract the candidate pavement portion for raveling detection;
- Computation of each subsection with the newly developed feature set for raveling analysis. Each 3D pavement data file covers a 5-m pavement section that is divided into six subsections;
- Raveling classification using Random Forest models, a supervised leaning technique with the known raveling classification as the learning samples;
- Post-processing to smooth isolated subsections in the six subsection-based raveling classification outcomes for determining the raveling severity level; and
- Aggregation of the detection outcomes to segment-level raveling measurement (e.g., normally 1 mile long), and report the raveling condition, including percentage and severity level, at the segment level based on highway agencies' survey practices.

Without loss of generality, the developed algorithms have been tested and validated using the pavement condition survey protocol in the Georgia Department of Transportation (GDOT). The algorithms can be extended to other highway agencies' pavement condition survey protocols by re-training the classification components using corresponding ground truth data. The algorithms were comprehensively tested and validated on I-85 and I-285 near Atlanta, Georgia. The 3D pavement data were collected on four test sections on I-85 (each of which is 1 mile long) and on the entire outer lane of asphalt pavement (61 miles) on I-285 for validation and testing. The testing results on I-85 showed that the developed algorithms are very promising for GDOT's use. The automatic classification results on each of the test sections were compared with the ground truth (the ones carefully measured by GDOT pavement experts). The predominant severity levels (Severity Level 1, 2, or 3) for Test Sections #1 and #2 are correctly classified. For Test Sections #3 and #4, there is, essentially, no raveling, and the classification errors are 0.93% and 0.31%. The testing on I-285 showed promising results for automatic raveling detection, classification, and measurement. All the pavements (with or without raveling) were 100% correctly detected and classified at the segment level (each segment is 1mile long). Because of the difficulty of correctly rating all the raveling areas using videolog images and 3D pavement data and the impact of cracking and flat-tire scratches, the raveling extent (percentage) showed a certain level of variation in comparison with the manually labeled ground truth. The differences between the surveyed results by the experienced GDOT pavement engineers and the automatically detected and measured results are less than 15%, and most of them are less than 10%.

In summary, the proposed algorithms have demonstrated promising capabilities to automatically detect and measure asphalt pavement raveling. Using the proposed algorithms will, potentially, save tremendous amounts of manual effort in field surveys, improve data accuracy, and help highway agencies make more informed decisions on pavement maintenance and rehabilitation. The developed algorithms are based on 3D pavement data that had been already collected (in this case, for automatic rutting and cracking data collection). Thus, using the same data collected for extracting other types of distresses will save great amounts of time and money by eliminating the need to make additional effort for data collections. The research outcome of this study will have a significant impact on state transportation agencies and industry by reducing the time and money spent on collecting asphalt pavement raveling data.

1 IDEA PRODUCT

The product of this IDEA concept exploration research project includes the algorithms developed to automatically detect, classify, and measure asphalt pavement raveling using three-dimensional (3D) pavement data obtained from 3D line laser imaging technology (for brevity, 3D laser technology). The proposed method includes five major components: (1) data pre-processing to remove data outliers, detect pavement markings and edge drop-off, and extract the candidate pavement portion for raveling detection; (2) computation of each subsection with feature set for raveling analysis; each 3D pavement data file covers a 5-m pavement section that is divided into six subsections; (3) raveling classification using Random Forest models, a supervised leaning technique with the known raveling classification as the learning samples; (4) post-processing to aggregate the six subsection-based raveling classification outcomes for determining the raveling severity level; and (5) aggregation of the detection outcomes to measure and report the raveling condition, including percentage and severity level, at the segment level based on highway agencies' survey practices; normally, a segment level is 1mile long.

The proposed algorithms were developed and validated using the raveling severity levels defined by the pavement condition survey protocol used by the Georgia Department of Transportation (GDOT) and can be extended to other state DOTs' protocols by re-training the classification components using corresponding ground truth data. The proposed algorithms were built based on the commonly used 3D pavement data that had already been collected (in this case, for automatic rutting and cracking data collection). Using common, already-collected data for raveling detection could save great amounts of time and money by eliminating or reducing the need for separate field data collections. The research outcome of this study has a significant impact on state transportation agencies and industry in that it can reduce time and money spent on collecting asphalt pavement raveling data.

2 CONCEPT AND INNOVATION

Raveling is defined as the "wearing away of the pavement surface caused by the dislodging of aggregate particles and loss of asphalt binder" in the distress identification manual for the long-term pavement performance (LTPP) program (FHWA 2014), and it is one of the most common asphalt pavement distresses that occur on U.S. highways. Figure 1 shows that raveling can occur on interstate highways and non-interstate roads. Raveling will increase pavement roughness, which results in poor ride quality and road and tire noise. Besides safety concerns, including loose stones that can break windshield glass and cause hydroplaning, raveling will shorten pavement longevity. For example, interstate highway I-285 in Atlanta, Georgia, has experienced severe raveling issues. Internationally, practitioners from the Netherlands and the United Kingdom (UK) found that for porous pavements paved on the Dutch trunk network (70% were paved with porous asphalt) or the hot rolled asphalt (HRA) wearing course paved on UK motorways, raveling is the predominant distress. If the raveled asphalt pavement is not sealed on time, the raveling problem could develop quickly. Roadway surface layers should be replaced quickly after the first observation of raveling (Miradi 2004). Thus, it is very crucial to identify raveling and treat it at its very early stage using low-cost, surface coating methods. Otherwise, much more expensive corrective treatments will be needed, which would seriously deplete highway agencies' already limited budgets.

FIGURE 1 Raveling on interstate highway and non-interstate road.

Although it is crucial to identify and treat raveling in its early stage, the commonly used manual survey method has hindered the early discovery of pavement raveling for the following reasons: (1) the manual survey process is very time-consuming, and it is impractical for highway agencies to conduct a full-coverage survey; (2) the survey protocol is very subjective, and survey results vary from rater to rater; (3) for high-traffic volume interstate highways, a raveling survey is often omitted by highway agencies due to the high demand of traffic control; and (4) a digital-image-based survey is unreliable because raveling is the change of pavement surface texture, and its appearance is susceptible to ambient lighting conditions. Although there are algorithms developed to automatically detect and classify raveling, they have not been thoroughly validated using the large-scale, real-world data. Thus, it is still difficult for transportation agencies to implement any of these algorithms. Therefore, there is an urgent need to develop objective, reliable algorithms for automatic pavement raveling detection, classification, and measurement.

The innovation of the proposed algorithms lies in the following two aspects:

1) Past studies using point-based laser profilers for pavement surface data collection cannot cover the pavement condition on the full lane; therefore, they were not reliable enough. The emerging 3D laser technology can reliably capture 3D pavement surface texture data with full lane coverage. This has brought new opportunities for developing more accurate and reliable algorithms for automatic pavement condition surveys. Though some raveling detection algorithms using 3D pavement data have been developed in academia [e.g., Mathavan et al. (2014)] and by industry (e.g., LCMS), they have not been fully

validated using a large-scale data set. In addition, these algorithms only dealt with raveling detection; raveling classification was not included, which should be based on highway agency protocols (e.g., raveling severity levels). Some other algorithms were developed to classify raveling. However, in those studies point-based laser profiles were used and only mean profile depth (MPD) or root mean square texture (RMST) was used for correlation. To the best of our knowledge, we are the first to develop comprehensive algorithms for both raveling detection and classification using 3D pavement data and also comprehensively test and validate the developed algorithms using a highway agency's protocol and real-world, large-scale dataset. In this research, the 3D pavement data were captured by highly precise and dense 3D laser systems that can capture continuous pavement transverse profiles at highway speed with 1 mm transverse resolution and 5 mm longitudinal resolution (driving direction). The depth precision is about 0.5 mm. Sponsored by the U.S. Department of Transportation Office of the Assistant Secretary for Research and Technology (USDOT/OST-R), the Principal Investigator and his research team (Tsai and Li 2012; Tsai et al. 2015) have used the full-lane-coverage 3D pavement data to improve the detection and measurement of pavement cracking and rutting. A sensing van has been developed and is now being used at Georgia Tech; the van is equipped with a high-definition line laser imaging device that was used to capture 3D pavement surface macrotexture data in support of automatic raveling detection and classification.

2) A set of comprehensive algorithms based on Random Forest, a supervised machine learning technique, was developed for raveling detection and classification. To the best of our knowledge, we are the first to develop both raveling detection and classification algorithms based on 3D pavement data and a highway agency's raveling survey protocol. The developed algorithms include five components:
    - Data pre-processing to remove data outliers, detect pavement markings and edge drop-off, and extract the candidate pavement portion for raveling detection;
    - Computation of each subsection with the newly developed feature set for raveling analysis. Each 3D pavement data file covers a 5-m pavement section that is divided into 6 subsections;
    - Raveling classification using Random Forest models, a supervised leaning technique with the known raveling classification as the learning samples;
    - Post-processing to smooth insolated subsections in the six subsection-based raveling classification outcomes for determining the raveling severity level; and
    - Aggregation of the detection outcomes to segment-level raveling measurement (e.g., normally 1 mile long), and report the raveling condition, including percentage and severity level, at the segment level based on highway agencies' survey practices.

Without loss of generality, the developed algorithms have been tested and validated using the pavement condition survey protocol in GDOT. The detected and classified raveling data can be the direct input to GDOT's pavement condition survey database, and used by its pavement management system.

3 INVESTIGATION

This section is organized into four subsections. The first subsection reviews the current practices of highway agencies for asphalt pavement raveling surveys; the second subsection reviews the state-of-the-art of algorithms for automatic raveling detection and classification; the third subsection presents the developed raveling detection and classification algorithms; and the last subsection presents case studies for algorithm testing and validation.

3.1 REVIEW OF CURRENT PRACTICE ON ASPHALT PAVEMENT RAVELING SURVEY

Because raveling is one of the most common asphalt pavement distresses, raveling data are collected by highway agencies for evaluating pavement conditions and determining proper treatments. Though raveling is defined in almost the same way by different highway agencies, rating methods of its severity levels and extents change from agency to agency. This subsection reviews the current practice in different agencies and summarizes the challenges and needs for improvement.

3.1.1 Raveling Definition

In the asphalt pavement condition survey manual used by GDOT, raveling is defined as the progressive disintegration of the surface layer (GDOT 2007). It is characterized by the loss of stones constituting the layer, which happens over time when the surface binder is eroded by friction from tires or when the pavement is damaged by an accident. It ranges from the loss of a few stones to the loss of an entire portion of the surface layer. Once the surface loses a few stones, adjacent stones break loose because they have no more support. Stones are then lost exponentially until the surface layer has disappeared and the lower layer lies bare. Raveling usually occurs in the wheel path and should not be confused with other types of distresses, such as cracks or potholes. Similar definitions can also be found in USDOT's distress identification manual (FHWA 2003) and manuals from other state DOTs (NYSDOT 2000; ODOT 2010).

3.1.2 Raveling Classification and Survey Practice

In highway agencies' practices, raveling is classified based on its severity, which is typically a qualitative definition. This can further be used for rating the overall pavement conditions and facilitate the determination of maintenance or rehabilitation treatments. The following summarizes the definitions of different raveling classifications and survey practices in various state DOTs:

1) Florida Department of Transportation (FDOT) (FDOT 2015)

Raveling is classified into three categories: low, moderate, and severe. Only significant areas of raveling are considered. An isolated area is not counted in a long section if it is not representative of the rated section. The predominant severity level and percent affected area of raveling are recorded. FDOT's definitions of different severity levels are as follows:

- **Light**: The aggregate and/or binder has begun to wear away but has not progressed significantly, with some loss of aggregate.
- **Moderate**: The aggregate and/or binder has worn away, and the surface texture is becoming rough and pitted; loose particles generally exist; loss of aggregate has progressed.
- **Severe**: The aggregate and/or binder has worn away and the surface texture is very rough and pitted; loss of aggregate very noticeable.

2) Georgia Department of Transportation (GDOT) (GDOT 2007)

Raveling is classified into Severity Levels 1, 2, and 3 based on the different raveling conditions. The following are the definitions:

- **Level 1:** loss of a substantial number of stones [see Figure 2(a)].
- **Level 2:** loss of most of the surface [see Figure 2(b)].
- **Level 3:** loss of substantial portion of the surface layer (>1/2 depth) (see Figure 2(c)].

In field surveys, raveling is closely observed, and an estimate (to the nearest 5%) is made of the extent and the predominant severity of the distress within the rated segment. The percent of the length of the rated segment (mile or partial mile) that contains raveling is recorded along with the predominant severity level. On two-lane and multi-lane undivided highways, the rater should determine which lane is in the worst general shape and base his or her estimate of the extent and severity of the pavement distress on what is observed in the lane selected. Likewise, on divided highways, only the lane in the worst condition in a given direction is to be rated; each direction is rated separately for divided highways.

(a) Severity Level 1 (b) Severity Level 2 (c) Severity Level 3

FIGURE 2 Raveling classification in GDOT (GDOT 2007).

3) Minnesota Department of Transportation (MnDOT) (MnDOT 2000)

The raveling classification in MnDOT is similar to the one in FDOT and is categorized as low, moderate, and high as follows:

- **Low:** The aggregate or binder has begun to wear away, but has not progressed significantly. Some loss of fine aggregate is visible.
- **Moderate:** Aggregate and/or binder has worn away and the surface texture is becoming rough and pitted. Loose particles exist, and there is loss of fine aggregate and some loss of coarse aggregate.
- **High:** Aggregate and binder have worn away, and the surface texture is very rough and pitted due to the loss of coarse aggregate.

4) Nebraska Department of Roads (NDOR) (NDOR 2002)

The terms for raveling classification in NDOR are the same as those in MDOT. However, the definitions are slightly different as follows:

- **Low**: Minimal loss of aggregate or binder [see Figure 3(a)].

- **Moderate**: Some aggregate loss; small areas may be stripped away [see Figure3(b)].

(a) Low (b) Moderate (c) High

- **High**: Sections greater than one square foot may be pitted stripped or eroded away [see Figure 3(c)].

(a) Low (b) Moderate (c) High

FIGURE 3 Raveling classification in NDOR (NDOR 2002).

5) Oregon Department of Transportation (ODOT) (ODOT 2010)

Again, the terms for raveling classification in ODOT are same as those in MDOT. However, the definitions are more quantitative and based on the percentage of aggregate loss as follows:

- **Low**: The aggregate has worn away resulting in 25% to 50% aggregate loss in a 1ft wide longitudinal strip of pavement surface [see Figure 4(a)].
- **Moderate:** The surface texture is noticeably rough and/or pitted with 50% to 75% aggregate loss in a 1-t-wide longitudinal strip of pavement surface [see Figure4 (b)].
- **High:** The surface texture is very rough and/or pitted with 75% or more aggregate loss in a 1-t-wide longitudinal strip of pavement surface [see Figure 4(c)].

In field surveys, raveling can be identified by a roughened or pitted texture on the pavement surface. Mechanical abrasion from tire chains, studs, snowplows, or dragging equipment that can significantly roughen the texture should be rated as raveling. Raveling tends to be most often found in the wheel paths, but can be elsewhere on the pavement surface. To measure raveling, the number of linear feet for each severity level in each path (inside, outside, and between wheel paths) must be recorded.

(a) Low (b) Moderate (c) High

FIGURE 4 Raveling classification in ODOT (ODOT 2010).

6) Texas Department of Transportation (TxDOT) (TxDOT 2009)

In TxDOT's pavement condition survey manual (TxDOT 2009), raveling is classified into low, medium, and high based the percentage of raveled area as follows:

- **Low**: The percent of raveled pavement area is from 1% to 10%.
- **Medium:** The percent of raveled pavement area is from 11% to 50%.
- **High:** The percent of raveled pavement area is greater than 50%.

7) Washington State Department of Transportation (WSDOT) (WSDOT 1999)

The terms for raveling classification in WSDOT are same as those in TxDOT. However, the definition is not based on quantitative measures as follows:

- **Low:** The aggregate and/or binder have started to wear away but has not progressed significantly. The pavement only appears slightly aged and slightly rough [see Figure 5(a)].
- **Medium:** The aggregate and/or binder have worn away and the surface texture is moderately rough and pitted. Loose particles may be present, and fine aggregate is partially missing from the surface [see Figure 5(b)].
- **High:** The aggregate and/or binder have worn away significantly, and the surface texture is deeply pitted and very rough. Fine aggregate is essentially missing from the surface, and pitting extends to a depth approaching one half the coarse aggregate sizes [see Figure 5(c)].

In a field survey, raveling is measured or observed differently depending on whether the road surface is Bituminous Surface Treatment (BST) or Asphalt Concrete Pavement (ACP). Care should be exercised when rating chip sealed pavements, as they tend to look raveled because of the inherent nature of the chip seal surface. However, raveling in chip sealed pavements (loss of aggregate) actually results in a condition of excess asphalt and should be rated as flushing. In practice, the raveling severity and extent are both estimated and recorded. The extent of raveling is estimated and expressed relative to the surface area of the surveyed lane. Recommended ranges for estimated extent include:

- Localized —Patchy areas, usually in the wheel paths.
- Wheel path —The majority of wheel tracks are affected, but little or none elsewhere in the lane.
- Entire lane —Most of the lane is affected.

(a) Low **(b) Medium** **(c) High**

FIGURE 5 Raveling classification in WSDOT (WSDOT 1999).

3.1.3 Summary

Based on the above review on the current practice of highway agencies for raveling classification and survey procedures, the following summarize the major challenges and the needs for research on automatic raveling detection and classification:

1) Unlike cracking, raveling is the change of surface texture and could be continuously distributed. The survey procedure for raveling is tedious, time-consuming, and error-prone. For example, in GDOT raveling is surveyed by means of a windshield survey. Raveling appears different when it is observed from standing on the ground or from a moving vehicle. Also, it is difficult for one riding in a car to accurately measure raveling extent. Thus, though raveling is one of the most common and critical asphalt pavement distresses, it is difficult to measure by means of in-field visual inspection. There is an urgent need to develop an automatic method for detecting and classifying raveling with emerging sensing technology and machine learning theory.
2) The classification of raveling in all major highway agencies is defined as the purpose of in-field visual inspection, which is subjective. This will cause variations in survey data. Some state DOTs, such as ODOT and TxDOT, use a quantitative measure (e.g., percentage of raveled area or percentage of aggregate loss) for raveling classification. However, it is unclear about how to quantitatively measure percentage of raveled area or percentage of aggregate loss.
3) Raveling is the change of asphalt pavement surface texture due to the disintegration of coarse aggregates. Different pavement texture patterns can be observed on the different raveling severity levels, specified by transportation agencies. It develops quickly after it starts. Hence, it is critical for highway agencies to identify it in its early stage so that preventive maintenance treatments (e.g., fog seal) can be applied before it deteriorates to higher severity levels and require more expensive corrective treatments. For low severity levels of raveling, the appearance of roadway surface texture changes under different lighting conditions; therefore, classifying it accurately depends on how one observes it. Under direct sunshine, it is hard to recognize lightly raveled surfaces. Also, if one conducts a windshield survey in a moving vehicle at highway speed, it is hard to recognize low-severity raveling. Thus, visual inspection under natural lighting conditions is difficult for a raveling survey, especially for low severity level raveling. To overcome this shortcoming, using 3D pavement data is a better alternative for capturing pavement surface texture because it is independent of ambient lighting conditions and can be accurately collected at highway speed. Thus, raveling data extracted from 3D pavement data is more reliable than the one collected visually under ambient lighting conditions.

3.2 REVIEW OF ALGORITHMS FOR AUTOMATIC RAVELING DETECTION AND CLASSIFICATION

Before the proposed algorithms for automatic raveling detection and classification are presented, the state-of-the-art practices of the existing methods are reviewed as follows.

3.2.1 Sensing Data for Raveling Detection and Classification

Due to the merit of being independent from ambient lighting conditions, laser sensors were used for collecting pavement surface texture data. Ooijen et al. (2004) started to use laser data [3.2 m Field of View (FOV), 25 points per scan] in detecting and classifying raveling. Since then, laser sensors with increasing FOV and resolution have been applied in raveling detection and classification. McRobbie et al. (McRobbie and Furness 2008; Scott et al. 2008; McRobbie et al. 2012) used laser data with 3.6 m FOV and 25 points per scan. Laurent et al. (2012a, b) worked on range data with 4 m FOV and 4,096 points per scan. Mathavan et al. (2014) presented a method to detect raveling from 3D pavement image (intensity and range).

3.2.2 Algorithms

Ooijen et al. (2004) developed the "Stoneway" algorithm to detect raveling on porous asphalt pavement. The Stoneway model calculates the percentage of lost stones per meter. The idea is that if somewhere on the surface there is a Stoneway, it will show up on the texture profile in one way or another. Two main parameters in the model are the height and the length of a gap (i.e., the imprint of a lost stone), which are referred to as the "highgap" and "greatgap," respectively. Furthermore, the severity of raveling is classified by the percentage of aggregate missing on the surface.

In this method, the raveling regions are defined as those gaps in the longitudinal sampling data that are large and deep (shown in Figure 6). Due to the nature of 25-line laser sensing, the method runs in one dimension per line. The parameter "greatgap" is used as the threshold between large and small. The other one, "highgap," is used to help judge if the gap is deep enough.

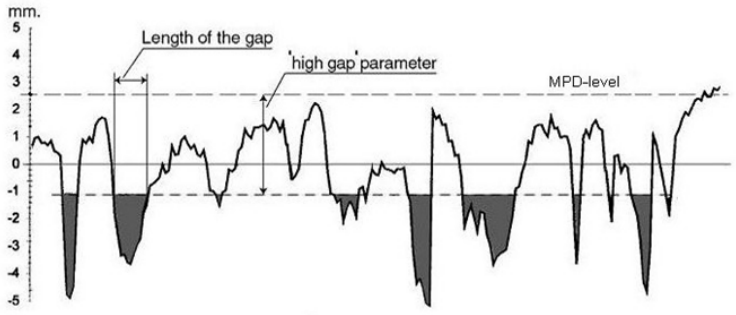

FIGURE 6 Stoneway algorithms (Ooijen et al. 2004).

Validation was performed in a test in which two datasets consisting of the Visual Condition Survey (VCS) data and the Stoneway data were correlated. The VCS method does not assess the actual amount of raveling; rather, it estimates the intervention year directly during the survey. Therefore, the comparison was held on the intervention year predicted by two approaches.

About 500 sections, each 100 m long, of different age classes and of the same age class but with differing severities of raveling, were chosen to validate the Stoneway derived intervention years and derived by applying the SHRP-NL propagation model against the direct VCS estimated year of intervention**.** Note that the testing data were from a porous asphalt surface.

As the validation result, analyses of standard deviations were run on both outputs. The result, Stoneway/SVCS = 0.87, suggests that the standard deviation of the Stoneway model is significantly smaller than the VCS standard deviation.

The second comparison was run on the means of the estimated intervention years. From the results shown in Figure 7, it can be seen that the Stoneway model tends to schedule the intervention later than the VCS estimation, except for the first planned years.

Standard deviations (years) degrees of freedom		Intervention year according to last monitoring cycle (2001)		
Increasing age	Construction year	2005-2006	2004	2001-2003
	1989-1992	0.88 140	0.52 138	0.52 140
	1993-1996	0.64 140	0.55 136	0.72 146
	1997-2000	0.59 76	0.73 98	0.29 8
→		increasing distress		

Table 1 Standard deviations of intervention years according to VCS

Standard deviations (years) degrees of freedom		Intervention year according to last monitoring cycle (2001)		
Increasing age	Construction year	2005-2006	2004	2001-2003
	1989-1992	0.44 140	0.57 138	0.81 140
	1993-1996	0.56 140	0.50 138	0.58 146
	1997-2000	0.61 76	0.26 98	0.37 10
→		increasing distress		

Table 2 Standard deviations of intervention years according to Stoneway-model

FIGURE 7 Results of comparison between "Stoneway" and VCS methods (Ooijen et al. 2004).

Two challenges are observed for the Stoneway method. First, the road surface is assumed to be flat in the horizontal direction; therefore, it may not work on inclined surfaces. Second, the sampling rate of the road profile is quite low. The transverse sampling rate is 500 mm per point. Under such a low rate, the collected profile may not be sufficient to represent the whole surface; therefore, the overall raveling detection and classification results can be influenced.

Laurent et al. (2012a, b) developed a Raveling Index (RI) to quantify raveling. The RI is calculated by measuring the volume of aggregate loss (holes due to missing aggregates) per unit of surface area (square meter). The 3D line laser imaging technology was used for surface range data collection. This high-resolution 3D laser data allow for the detection of missing aggregates. The formula for RI estimation is given below:

$$RI = V_{ravelling}/A_{total}$$

Limited tests have been done on raveling detection. The general method used here is to perform raveling detection on the same road section repeatedly. If the results tend to be similar, then the robustness of the detection approach is proved (on a limited level, though). The results of a repeatability test (three passes) on road sections in the Netherlands are shown below (see Figure 8).

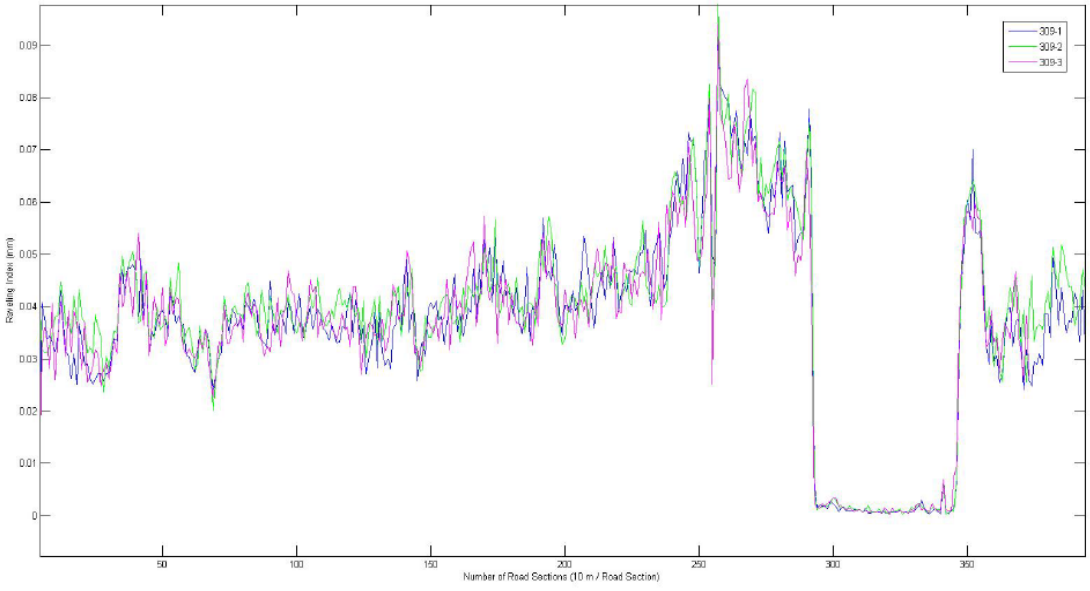

FIGURE 8 Repeatability test results (three passes in three different colors) (Laurent 2012a).

In addition, some visual comparison was carried out. By watching the RI on surfaces with different raveling severities, the RI seems to be relevant to raveling severity. A comparison figure is given below (shown in Figure 9).

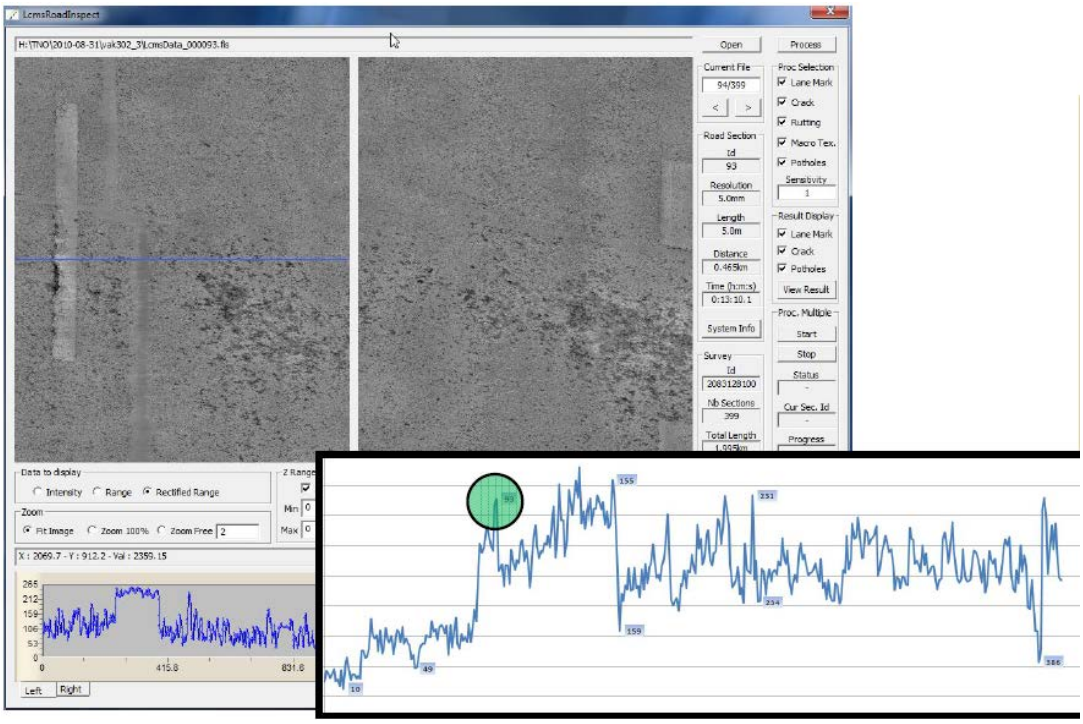

(a) LCMS data of pavement surface with high raveling index (RI).

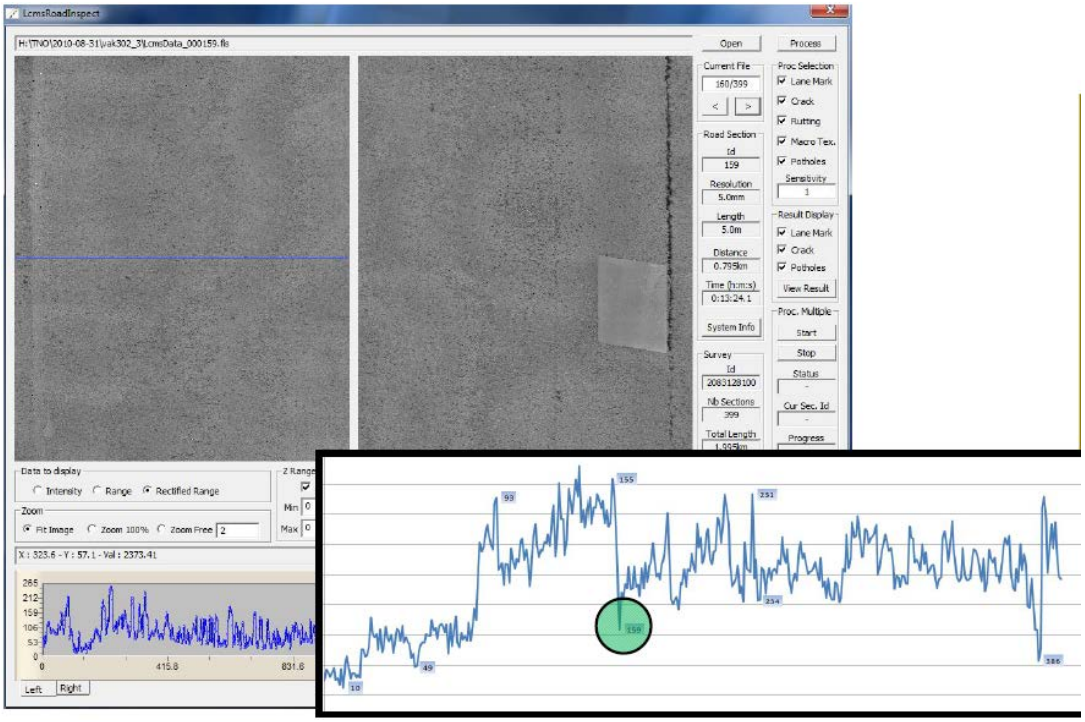

(b) LCMS data of pavement surface with low raveling index (RI).

FIGURE 9 Results comparison with different raveling index (RI) (Laurent 2012a).

Different from Ooijen et al. (2004), the density of 3D laser data used here was high enough to cover the entire lane transversely. Therefore, the performance of the raveling detection and classification was expected to be better. However, the tests for raveling detection are very limited and without systematic validation using a large-scale dataset.

McRobbie et al. developed two raveling detection and classification methods (McRobbie and Furness 2008; Scott et al. 2008; McRobbie et al. 2012). The first method is based on MPD (Scott et al. 2008). Locations that differ from the characteristic level by a sufficient depth and over a significant length are deemed to be raveled. The proportion of the road affected by raveling is reported. Two parameters used here are *D* (the required difference that must be observed between the baseline and the filtered profile before fretting can be reported) and *L* (the length of profile over which *D* must be exceeded before fretting can be reported).

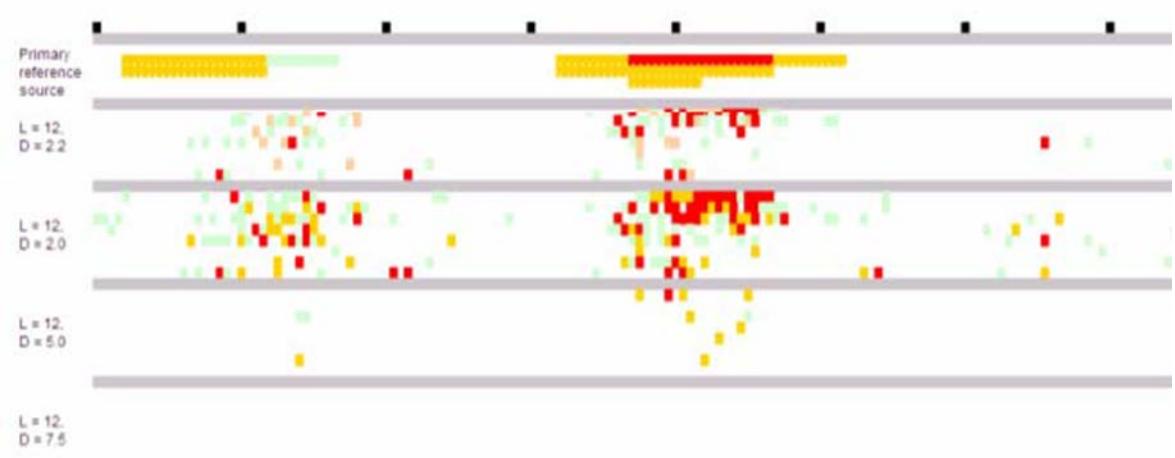

FIGURE 10 Visual representation of surface using root mean square texture (RMST) (McRobbie and Furness 2008).

In the second approach, RMST was calculated and reported (McRobbie and Furness 2008; McRobbie et al. 2012). By assigning a color to each of the RMST values in the data, it was possible to produce a visual representation of the surface texture in which features such as road markings, metalwork, surface changes, potholes, and raveling could be seen (see Figure 10). Based on RMST, a raveling detection algorithm is introduced. The basic underlying concept for the algorithm is the comparison of the distribution of RMST values in a small ("Local") area against those from a much larger surrounding ("Global") area (see Figure 11).

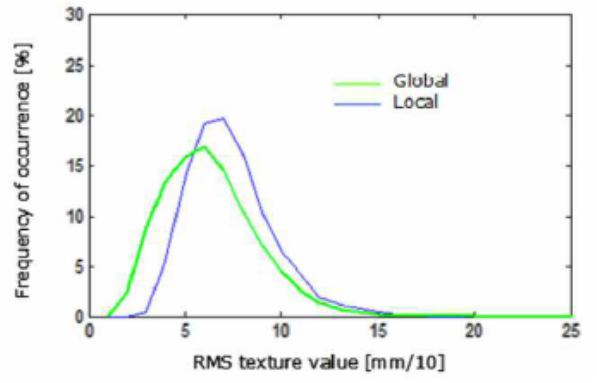

FIGURE 11 An example of distribution difference between "Local" area and "Global" area (McRobbie and Furness 2008).

To provide a good range of reference (i.e., ground truth) data, a group of sites totaling approximately 90 km was selected (see Figure 12), representing a combination of different surface types (thin surface course, porous asphalt, hot rolled asphalt, etc.) and surface conditions. Then, the coarse visual inspection (CVI) method was proposed as a suitable means of collecting larger volumes of reference data using a two-stage process:

- Stage 1 - Validation and refinement of the driven survey methodology against a walked survey based on trial sites; and

- Stage 2 - Driven survey of approximately 100 lane km of network based on a mixture of surface types and surface conditions upon the successful completion of Stage 1.

Site	Description	Site lane length [m]
1	A28. Godmersham to Chilham	7102
2	A28. St. Michaels, Tenterden	6490
3	A228. Colts Hill to Hale Street Bypass	9227
4	A249. Detling to Stockbury	8985
5	A256. Betteshanger to Guston	9583
6	A259. Rhee Wall	5186
7	A2070. Rhee Wall to Kingsnorth, Ashford	14305
8	A299. Thanet Way	23621
9	A28/A268 Sandhurst to Newenden	5281
	Total length	89780

FIGURE 12 Sites selected for testing the RMST method (McRobbie and Furness 2008).

Figure 13 presents the output of RMST method (this is shown as a single value every 100 m) and the reference data (displayed as the sum of all weighted sum values within a 100 m length) on two validation datasets. This shows, generally, a good agreement; the same areas were usually picked out by higher values and a few areas in which the local trends and shapes of the lines followed each other well.

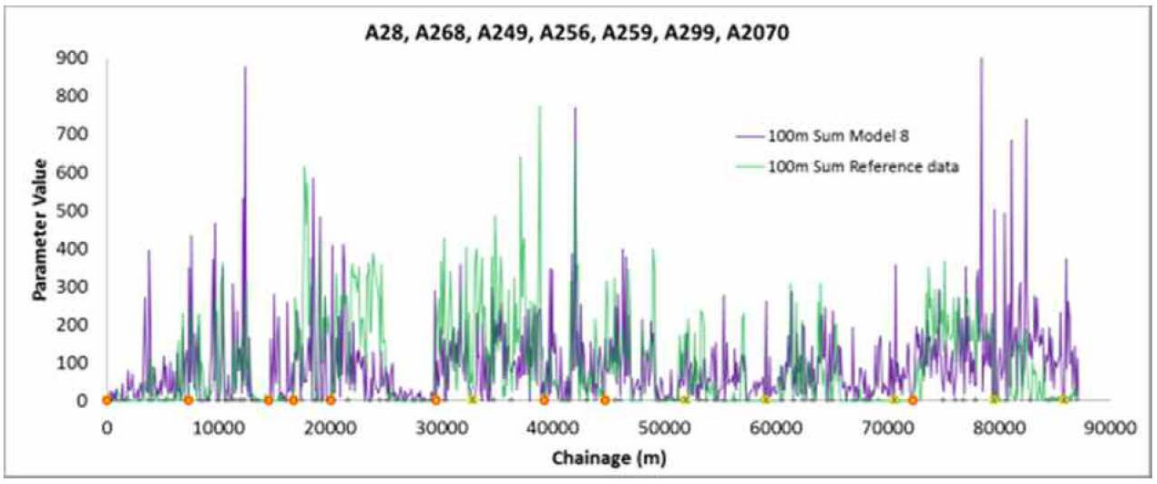

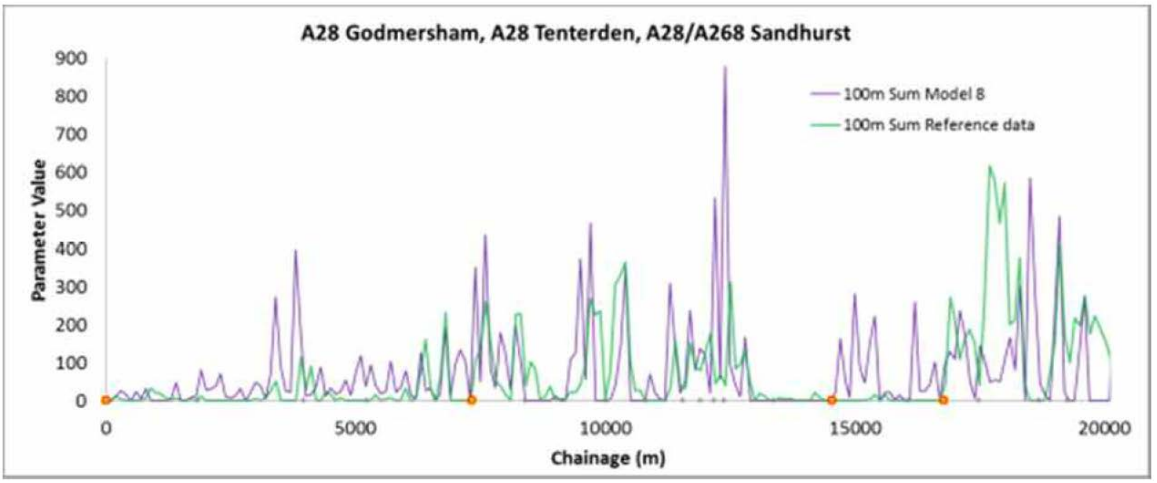

FIGURE 13 Results comparison between proposed method output and reference data (McRobbie and Furness 2008).

The first method, MPD, is an extension of the Stoneway method proposed by Ooijen et al. (2004). Similar to the Stoneway method, MPD suffers from its assumption that the surface should be horizontally flat. Though the baseline used in MPD is calculated on each relatively short length (e.g., 200 m), it still fails on surfaces with large inclines (obvious in short lengths). As for the second method, RMST, some challenges exist due to its basic assumption. The first one is how to determine local and global. The criteria should not be the same for different surfaces and under different road conditions. The other challenge is how to accurately estimate surface conditions based on the inaccurate representation; that is, an RMST histogram. Many different surface conditions may appear similar in the RMST histogram.

The aforementioned two methods are estimating absolute measurements of raveling condition. However, the estimation of the absolute raveling measurement is difficult and would require detailed knowledge of the surface material. Therefore, McRobbie et al. (2015) reported a method that estimates raveling condition in a relative manner. It is composed of two stages: (1) aligning 3D data collected from successive surveys, and (2) identifying the changes in surface condition among successive collected data. In the first stage, the profile data are aligned in two directions sequentially; first in longitudinal direction, then in transversal direction (Figure 14). After aligning 3D data, seven parameters are selected from 30 parameter candidates to detect changes in 3D pavement data (Figure 15).

For validation, the ground truth with various raveling conditions is collected in the lab, where a real pavement sample is worn by a MLPC rutting machine to simulate deteriorating raveling conditions. Then a large number of standard surface shape parameters are tested on the ground truth to determine if any of these could be used to quantify surface disintegration at any stage. In the end, there was a large degree of uncertainty in the reported results.

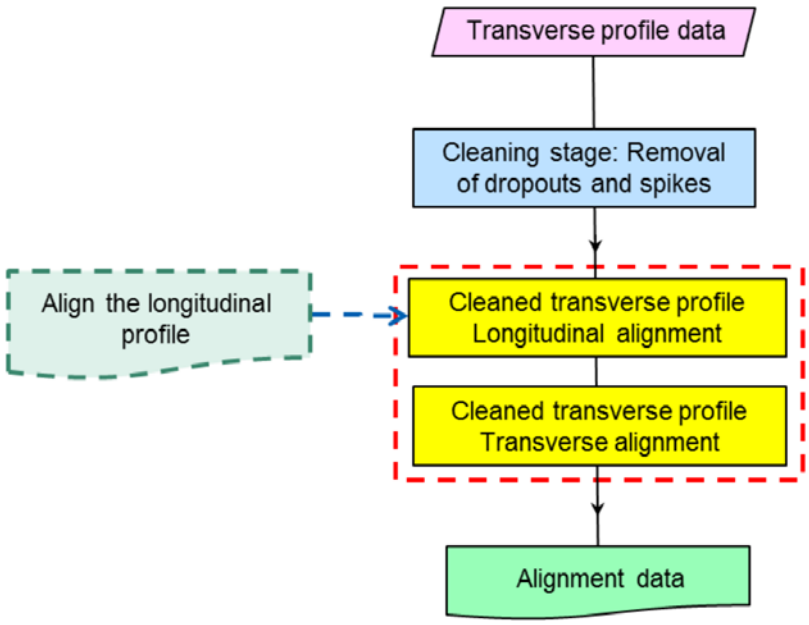

FIGURE 14 The framework of 3D data alignment (McRobbie et al. 2015).

Parameter name	Description
c1	Profile height defining volume in peaks – set to include top 10% by default.
c2	Profile height defining volume in valleys – set to include lowest 20% by default.
Vmp	Peak material volume of scale limited surface: Volume of material in the peaks of the sample, between 0% material ratio and material ratio p%, calculated in the zone above c1 $Vmp = \frac{K}{100\%}\int_{p}^{100\%}[Smc(p) - Smc(q)]dq$ Where K is a constant.
Vmc	Core material volume of the scale limited surface: Volume of material in the core, between two material ratios p and q, calculated in the zone between c1 and c2. Vmc = Vm(q) – Vm(p)
Sp	Maximum peak height.
Sr1	Upper material ratio.
Sr2	Lower material ratio.

FIGURE 15 Parameters used to indicate changes in aligned 3D pavement data (McRobbie et al. 2015).

Mathavan et al. (2014) presented a method to detect raveling from 3D pavement image (intensity and range). First, a texture descriptor method called Laws' texture energy measure is used in conjunction with the Gabor filter and other morphological operations to distinguish road areas from others. Then raveled road areas are detected by estimating STD on the corresponding range data. By heuristically setting the thresholds for STD values, the raveling condition (within a limited grid) can be characterized into good, average, or bad.

Their method was tested on 900 3D pavement images (intensity and range). According to the cases presented in the paper, their method successfully removed unwanted pavement areas, such as those with white markings, and rated the raveling condition for the rest of pavement areas. However, there is a lack of comprehensive validation in this paper. Detailed information on the validation dataset, such as the location of data collection, the distribution of raveling conditions in these data, are not mentioned in this paper. Moreover, the outcome of raveling quantification is not compared with any kind of ground truth (e.g., visual survey results). Therefore, there is still a gap between the practical raveling classification protocol used by transportation agencies and the method proposed by Mathavan et al. (2014).

3.2.3 Summary

First, most of the raveling detection and classification research is still at the research stage. Compared with the extensive studies for other pavement distresses; for example, cracking and rutting, there are only a very limited number of studies on raveling detection and classification.

Second, there are no global indicators that can be universally accepted for reliable raveling detection and classification. In addition, many indicators are based on certain assumptions about the surface that might not be applicable to other cases. For example, MPD, the commonly used indicator, employs two parameters to describe the volume of losing aggregates to classify raveling. However, it only works on horizontally flat surfaces due to the nature of its definition. Another indicator, RMST, relies on the concept that raveled areas have a different texture pattern than non-raveled ones. When applying RMST on a long stretch of consistently fretted pavement, this indicator might fail to identify the raveled areas.

Third, even with only a limited number of indicators that can be potentially used for raveling detection and classification, the existing methods frequently require parameter tuning and adjustment based on empirical experiment. These empirical trial-and-error approaches might constrain the existing algorithm from a broad application for different surfaces, different raveling conditions, or even different data sources.

Finally, most of the validation methods used in literature only contain a limited amount of data. More importantly, among the limited amount of data, the diversity of the data might not be adequate to objectively reveal the true performance of the automatic method (e.g., only on one or two2 types of pavement) or its limitations.

To summarize, automatic raveling detection and classification is still in its early stage of development. Some algorithms using 3D pavement data have been developed by academia and industry, but they only dealt with raveling detection. Some other algorithms dealt with raveling classification, but only point-based laser profiles were used. Thus, in this research, we developed comprehensive algorithms to consider both raveling detection and classification using GDOT's raveling survey protocol. More importantly, to make it possible for practical application, a large-scale testing and validation was conducted using the real-world 3D pavement data.

3.3 PROPOSED RAVELING DETECTION AND CLASSIFICATION ALGORITHMS

3.3.1 Introduction to 3D Laser Technology

As previously mentioned, digital images captured under varying ambient lighting conditions are not suitable for raveling detection because the ambient lighting has significant impact on the appearance of surface texture. With the advancement of sensing technology, 3D laser technology can capture high-accuracy and high-resolution 3D pavement data that preserve the fine granularity of 3D surface textures shown in Figure 16. Thus, the proposed raveling detection and classification algorithms based on 3D pavement data are expected to be more reliable and accurate.

Figure 17 shows the Georgia Tech Sensing Vehicle (GTSV) used for 3D pavement data collection. The GTSV was applied in the research project, *A Remote Sensing and GIS-Enabled Asset Management System* (Tsai and Wang 2013), sponsored by USDOT/OST-R. This vehicle is equipped with a 2D imaging system, a 3D laser system, a mobile Light Detection and Ranging (LiDAR) system, an Inertial Measurement Unit (IMU), and a Differential GPS. IMU and GPS systems establish very high-accuracy location references. Through the location references, 2D images and 3D laser data can be related to help establish the ground truth data. Unlike the laser profiler, collecting only two laser lines, the 3D line laser imaging system can capture 3D full-lane-width pavement surface data. There are 4,096 points at each transverse line, and the interval between two adjacent points is 1 mm. In the longitudinal direction, the interval between two adjacent transverse lines is 5 mm if the vehicle is operated at 100 km/h. Sample surface texture images are shown in Figure 17. The PI and his research team have used 3D pavement data to automatically detect and measure cracking (Tsai and Feng 2012; Jiang and Tsai 2015), rutting (Tsai et al. 2015), concrete joint faulting (Tsai et al. 2012), and micro-milling pavement surface texture quality control (Tsai et al. 2014). The PI has also been invited by the committee of TPF-5(299) of "Improving the Quality of Pavement Surface Distress and Transverse Profile Data Collection and Analysis" to present the 3D pavement data characteristics and the validation procedures developed to ensure 3D data quality (Tsai and Wang 2015).

3.3.2 Overview of Proposed Algorithms

The overall procedure for raveling detection and classification is as follows. First, 3D pavement image (5 m by 4 m in length and width) is divided into six subsections. Then, raveling detection and classification algorithms are applied on each subsection to detect and classify raveling. Based on GDOT's pavement condition survey protocol, raveling is classified as Severity Levels 0, 1, 2, and 3. Severity Level 0 means there is no raveling. After raveling is detected and classified in each subsection of a 3D pavement image, the raveling survey results can be aggregated for each 1-mile segment based on GDOT's pavement condition survey protocol. In GDOT, only the predominant severity level of raveling in each mile is recorded. It should be noted that the intermediate results shown in the above procedures can also be used to fit in with other highway agencies' survey protocols.

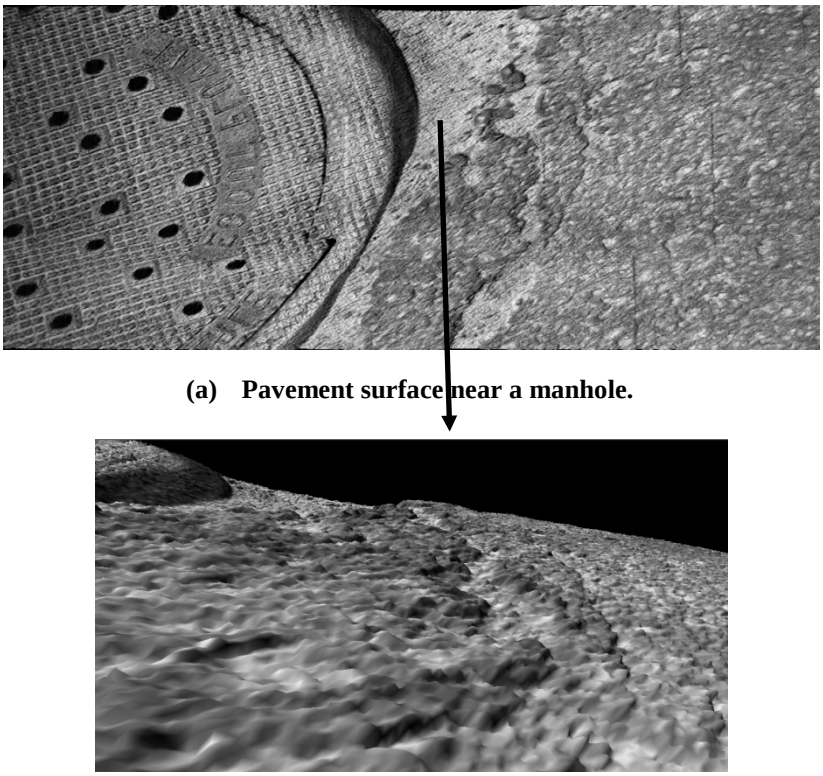

(a) Pavement surface near a manhole.

(b) A 3D close-out view of pavement surface.

FIGURE 16 Visualization of 3D pavement surface data.

FIGURE 17 Georgia Tech Sensing Vehicle.

Figure 18 illustrates the general framework of the proposed raveling detection and classification method. 3D pavement data are stored in individual files; each image covers a 5-m pavement section. To consider the non-uniformity of a 3D pavement image, it is divided into six equal-size subsections: three in each wheel path. The number of subsections in each wheel path is determined as a balance between two factors: the non-uniformity of raveling, and the manual rating effort. Each image is processed independently and outputs image-level raveling severity levels. This process is divided into the following four steps:

1) First, a detection algorithm quantifies raveling by outputting a set of features; that is, statistical characteristics of the pavement surface texture are calculated. These features are calculated after splitting the section into six subsections, three in each side of the lane.
2) Second, a properly trained classifier labels each subsection with a severity level (0, 1, 2, or 3), given the features calculated by the detection algorithm for that subsection. Severity Level 0 indicates no raveling.

Severity Levels 1 to 3 comply with GDOT's definitions of raveling severity levels.

3) Third, for each 3D pavement image, a single severity level is assigned based on a predefined aggregate rule.
4) The last step of the process is to aggregate the classified outcomes into one-mile segment-level ratings, which are compatible with GDOT's raveling survey protocol. For each segment, the percentage of each raveling level is generated, along with the predominant raveling level of the section.

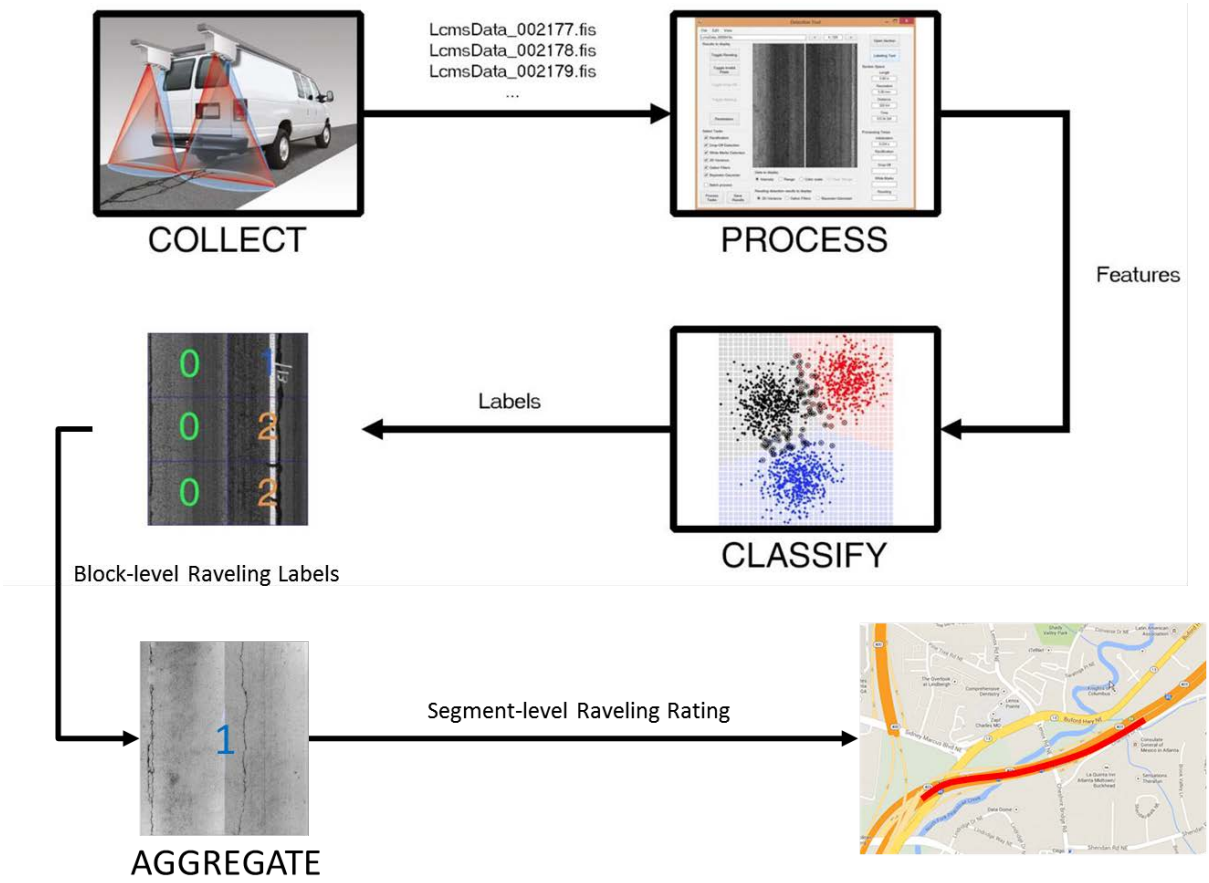

FIGURE 18 General framework of raveling detection and classification.

In the proposed algorithms, the most important step is to automatically classify raveling based on pre-defined pavement surface texture features. This is implemented by using a classification (or prediction) model. Figure 19 shows the procedures to find a prediction model. Finding a prediction model that accurately assigns a label to new data required us to manually label a significant number of examples (i.e., ground truth data).

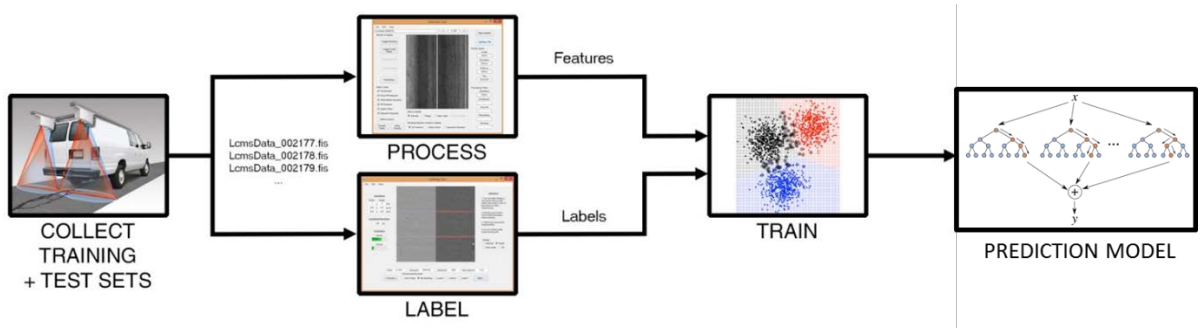

FIGURE 19 Methodology used to obtain classifiers.

3.3.3 3D Pavement Data Pre-Processing

Before the detection algorithms can be applied, the raw 3D laser data needs to be pre-processed. First, the invalid data points, which are indicated by invalid depth values in the data file (shown in Figure 20) should be removed. Second, pavement marking needs to be detected because only the portion between two pavement markings is used for raveling detection and classification. Because of their high reflectivity, pavement markings produce higher laser reflectance values, so they can be detected by using intensity data (a simple grayscale picture aligned with the 3D range data). The pixels in the pavement edge drop-off area are also removed because they might trigger false positives. Figure 21 highlights the detected pavement marking and edge drop-off in green.

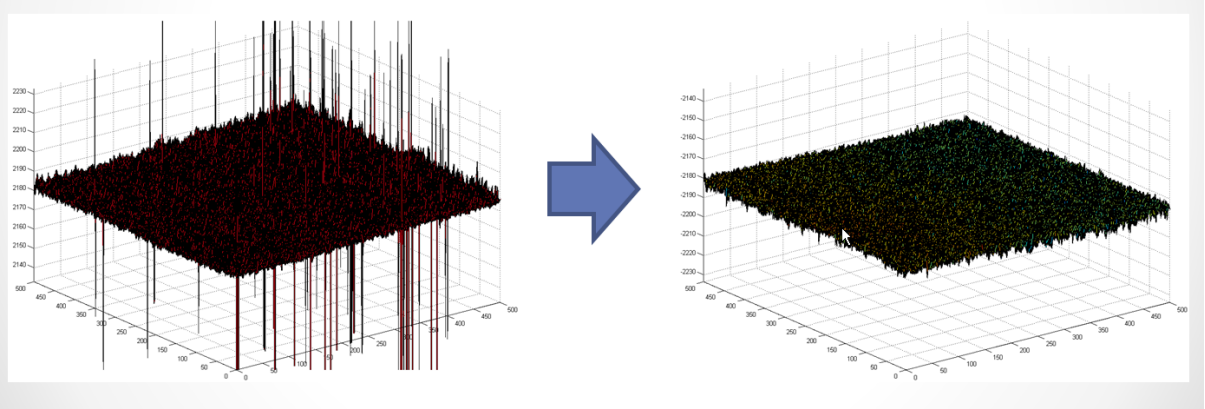

FIGURE 20 Removal of invalid data point.

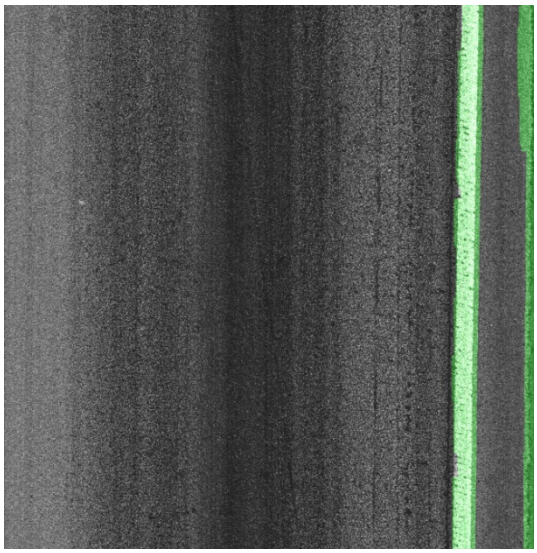

FIGURE 21 Pavement marking and edge drop-off detection.

Finally, the pre-processing algorithm rectifies the range data in order to eliminate the cross slope of the pavement. The curvature of the pavement surface can induce false positives and negatives. The rectification algorithm blurs the range image with a normalized box filter and subtracts the blurred image from the original. This operation removes the local mean from the data and makes edges and raveling easier to identify. Figure 22 illustrates this pre-processing step.

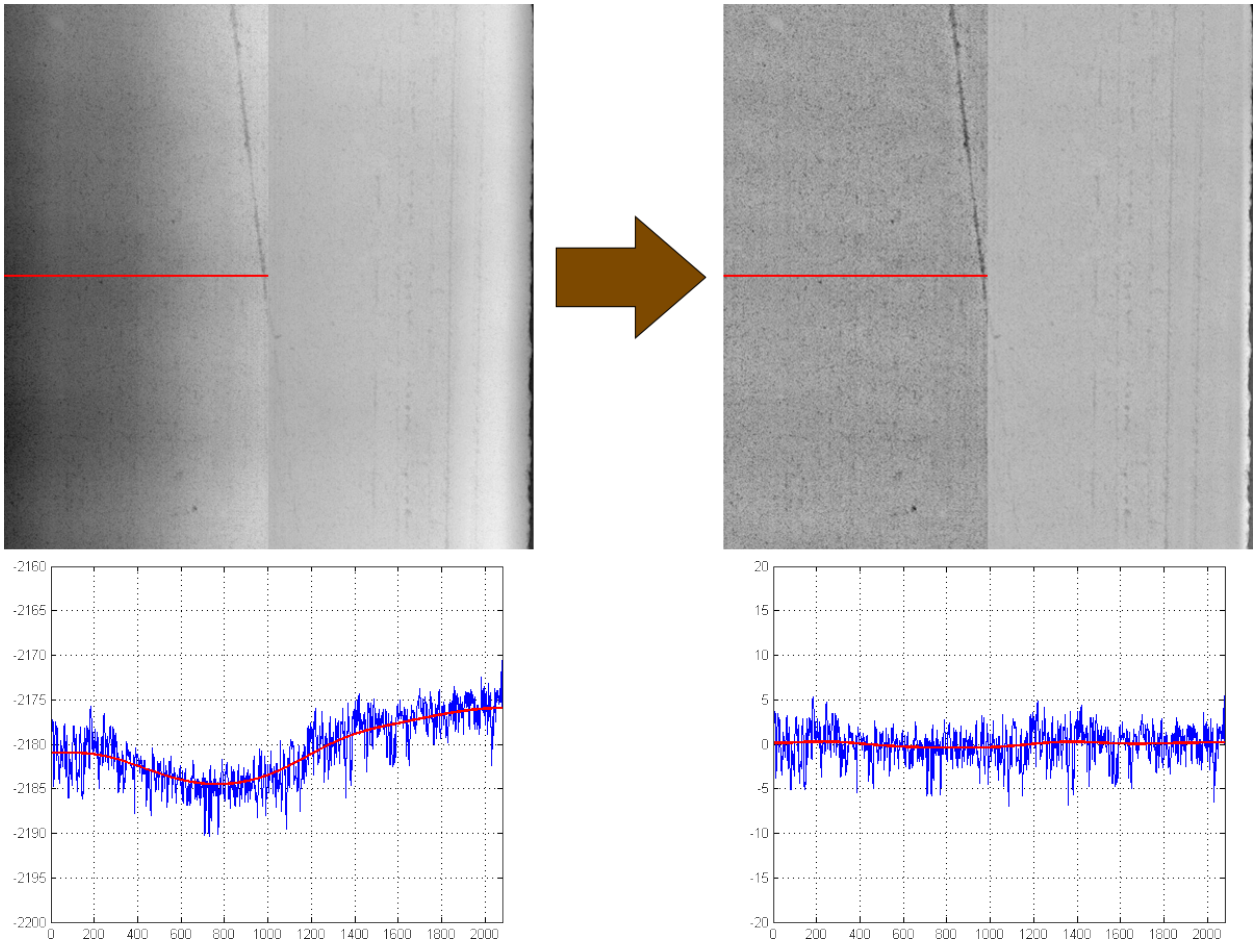

FIGURE 22 Before and after rectification of range data.

3.3.4 Raveling Detection Algorithms

As previously discussed, each 5-m pavement section, which is stored in a data file, is divided into six subsections, as shown in Figure 23. In each subsection, two types of statistical factors (i.e., features) are calculated based on the range data that indicate the pavement surface texture:

1) Pavement surfaces with light raveling (e.g., Severity Level 1) have the isolated aggregate loss. The distributions of range data collected on these surfaces will be less uniform than pavement surface without raveling. As the raveling conditions deteriorate to Severity Level 2, more aggregate loss occurs and gets channelized. Therefore, the distributions of range data become non-uniform. When the pavement surfaces have severe raveling (e.g., Severity Level 3), the distribution of range data on these surfaces will be uniform again (since the entire surface layer is lost). Thus, the selected statistical features need to capture the characteristics of surface texture changes under different severity levels of raveling. Based on our study, seven statistical features are selected and extracted from each subsection, as listed in Table 1.
2) To better capture the statistical characteristics of a raveled surface, the distribution of some indicators on all small patches of a subimage are approximated and applied as features. For example, the distribution of standard deviation values along all 0.1 m * 0.1 m patches within a subsection can be used to distinguish raveling levels 0 and 1 (as shown in Figure 24), which illustrates the distributions of standard deviation in subsections with class 0 (no raveling) and class 1 (Severity Level 1). The distributions of STD on raveled subsections are likely to expand wider than those of non-raveled subsections, which might be because the raveled surface is more non-uniform. The distributions are estimated for each one of the seven features mentioned above. Each distribution is discretely represented by a histogram with 100 bins. Therefore, in

total, 700 features are computed to capture the distributions of the seven defined features.

TABLE 1 Features Estimated on Range Data of Each Subsection

Feature	Physical Meaning	Dimension of Statistical Value	Dimension of Distribution
Standard deviation	Quantify the amount of variation or dispersion of range values on 2D pavement surface	1	100
Interquartile range		1	100
Arithmetic average of absolute values	Characterize the surface based on the vertical deviations of the roughness profile from the mean line	1	100
Root mean square		1	100
Skewness	A measure of symmetry, or more precisely, the lack of symmetry on the range values of 2D pavement surface	1	100
Kurtosis	A measure of whether the range values of 2D pavement surface are peaked or flat relative to a normal distribution	1	100
Aggregate loss volume	Directly estimate the volume of aggregate loss by differentiating range image with reference surface (assumed to have no raveling)	1	100

After summing up the two types of features, there are total of 707 features for each subsection. With such a large feature vector extracted from the range data, the key is to establish a relationship between the feature vector and the true raveling severity level, which will be presented next.

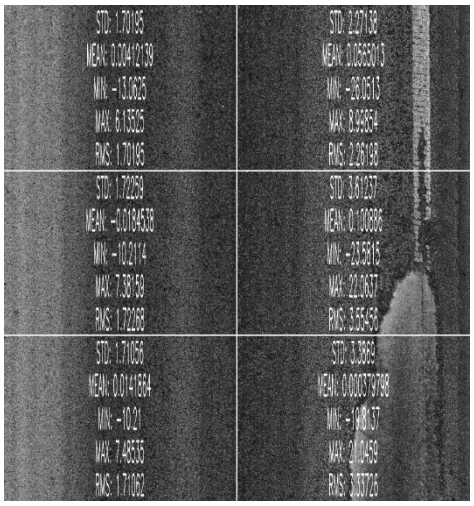

FIGURE 23 Statistical feature output for a pavement section.

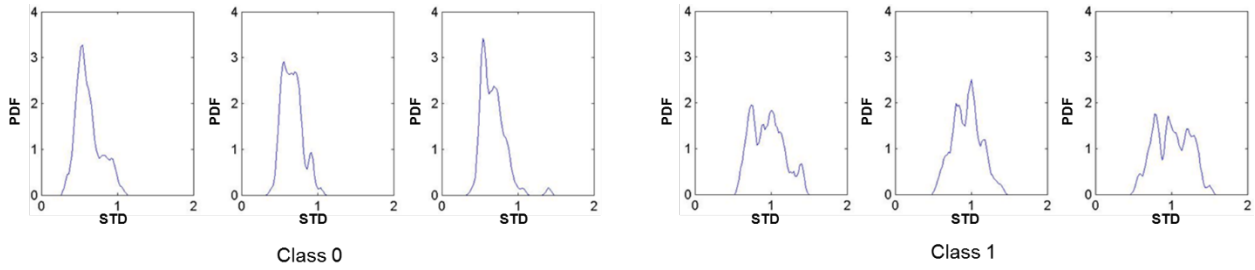

FIGURE 24 Distribution of indicators for pavement with different raveling level.

3.3.5 Development of the Raveling Classification Algorithms

According to GDOT's pavement condition survey protocol, raveling is classified as three types of severity levels (Level 1, Level 2, and Level 3). For convenience, we use Level 0 to indicate the conditions of no raveling. A supervised learning technique, Random Forest (RF), was adopted in the raveling classification algorithms.

In a supervised learning, a classifier is trained on a correctly (manually) labeled set (i.e., ground truth data). The numerical value corresponding to each labeled pavement subsection is called a feature. In the proposed algorithms, 707 statistical values form a feature vector for each subsection.

RF is used because it is one of the most commonly used supervised learning techniques (Breiman 2001; Cutler et al. 2007). It is an ensemble learning method for classification and regression that builds many decision trees at the training time and combines their output for the final prediction. RF corrects for the decision tree habit of over fitting to their training set, which is especially effective when there is a large dimension of features. Since the dimension of the feature vector for each pavement subsection is as high as 707, it is natural to take RF into consideration as one possible classifier. Meanwhile, two other widely used classification techniques, Support Vector Machine (SVM) and AdaBoost, were also evaluated and compared using a ground truth dataset with 23,467 feature vectors (15,118 vectors for raveling level 0; 5,091 for raveling level 1; 3,053 for raveling level 2; and 205 for raveling level 3). The evaluation results of all three classification techniques are listed below:

TABLE 2 Evaluation Results of AdaBoost Classification Technique on Raveling Ground Truth Dataset

Classified / ***Ground Truth***	**Class 0**	**Class 1**	**Class 2**	**Class 3**	**Precision**	**Recall**
Class 0	14,531	576	11	0	0.961	0.933
Class 1	1,014	3,388	689	0	0.665	0.833
Class 2	5	97	2,951	0	0.966	0.772
Class 3	25	8	172	0	0	0

TABLE 3 Evaluation Results of SVM Classification Technique on Raveling Ground Truth Dataset

Classified / ***Ground Truth***	**Class 0**	**Class 1**	**Class 2**	**Class 3**	**Precision**	**Recall**
Class 0	14,757	359	0	2	0.976	0.956
Class 1	653	4,129	304	5	0.811	0.878
Class 2	3	208	2,817	25	0.923	0.897
Class 3	19	4	19	163	0.795	0.836

TABLE 1 Evaluation Results of RF Classification Technique on Raveling Ground Truth Dataset

Classified / ***Ground Truth***	**Class 0**	**Class 1**	**Class 2**	**Class 3**	**Precision**	**Recall**
Class 0	14,756	375	1	4	0.976	0.961
Class 1	577	4,169	327	2	0.819	0.869
Class 2	3	241	2,791	16	0.914	0.888
Class 3	15	11	24	155	0.756	0.876

From the precision and recall rates listed above, we can see that the performance of SVM and RF are both much better than the AdaBoost classification. Based on the fact that most of the asphalt pavements have no raveling and the rest of them have mostly with level 1 raveling, the number of misclassification cases between Class 0 (no raveling) and Class 1 (level 1 raveling) provide us a hint for the comparison between SVM and RF. RP slightly outperforms SVM in terms of the misclassification cases between Class 0 and Class 1 (577 + 375 = 952 vs. 653 + 359 = 1012). Therefore, RF is selected as the classification technique in our raveling classification algorithm. Figure 25 shows the training process of a RF.

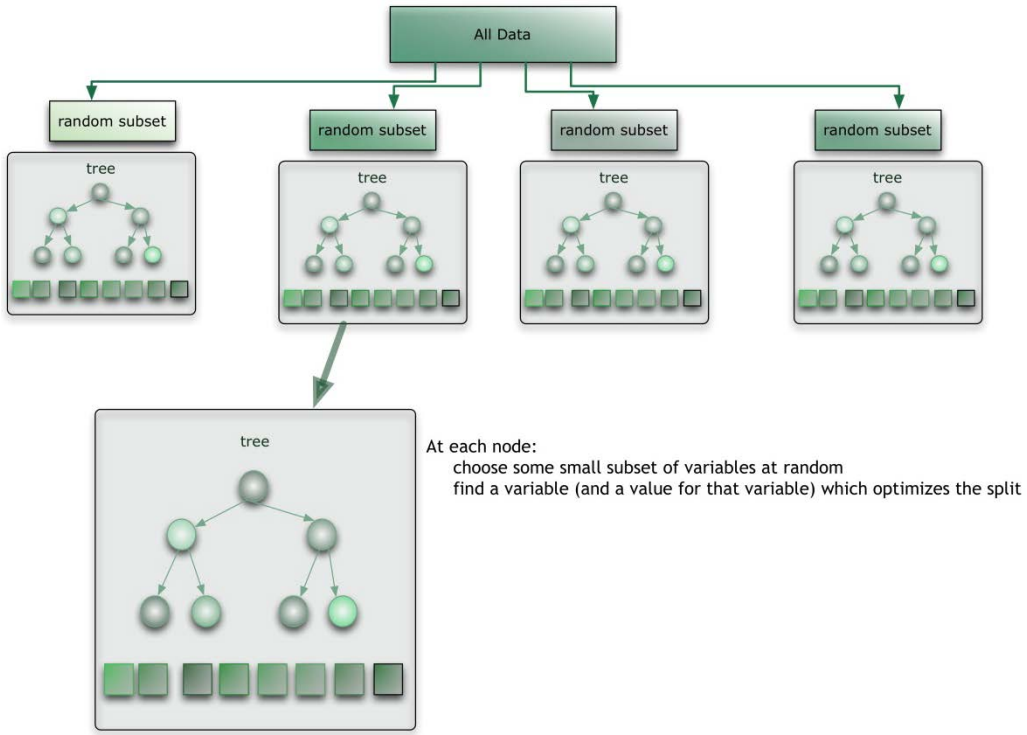

FIGURE 25 Training process of a Random Forest (Benyamin 2012).

3.3.6 Development of the Raveling Aggregation Algorithms

This section develops an aggregation method with algorithms to mimic and automate GDOT's current raveling survey protocol for the recording at each segment (~1 mile). The raveling aggregation might be adjusted slightly based on different state DOT practices in the implementation. Erroneously classified subsections can be identified and removed by checking isolated subsections based on the assumption that raveling pavements are continuous to some certain extent. In addition, a small spot of raveling (e.g., raveling in an isolated subsection) is normally neglected in a practical survey, which would not affect the decision making on network-level pavement maintenance. Therefore, in the proposed aggregation method, an isolated subsection with raveling is not to be counted at the segment level. Based on the extensive discussion with GDOT's engineers, the aggregation algorithms were developed to aggregate the subsection-level raveling into the one at the segment level. The algorithms are divided into two phases: the first phase removes outliers, such as the isolated subsection with raveling, and the second phase smooths the raveling distribution. Finally, the outcomes are aggregated to a 1-mile segment to support GDOT's pavement management system. The following describes the steps for outlier removal:

1) For a given subsection, compare its assigned severity level with the severity levels of its direct neighbors.
2) Each subsection has five neighbors, as shown in Figure 26. A neighbor can be in the next or previous image. For subsections at the boundary (first and last image), there are only three neighbors instead of five.
3) If the severity level of the subsection is isolated among its neighbors (e.g., Level 1 surrounded by five at Level 0) then change the severity level to the majority severity level in the neighbors.
4) Repeat the above steps for all subsections. Figure 27 shows an example of outlier removal.

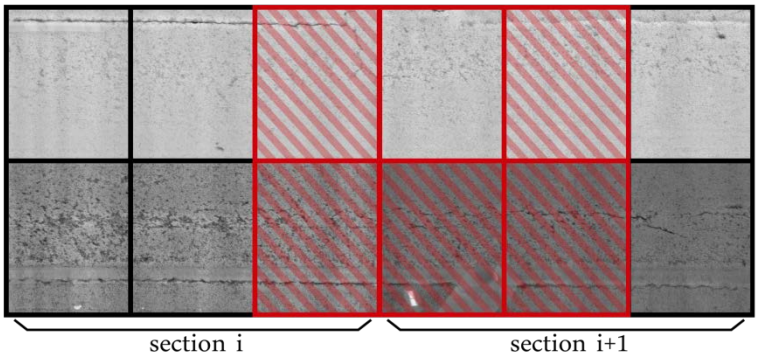

FIGURE 26 Subsection and its neighbors.

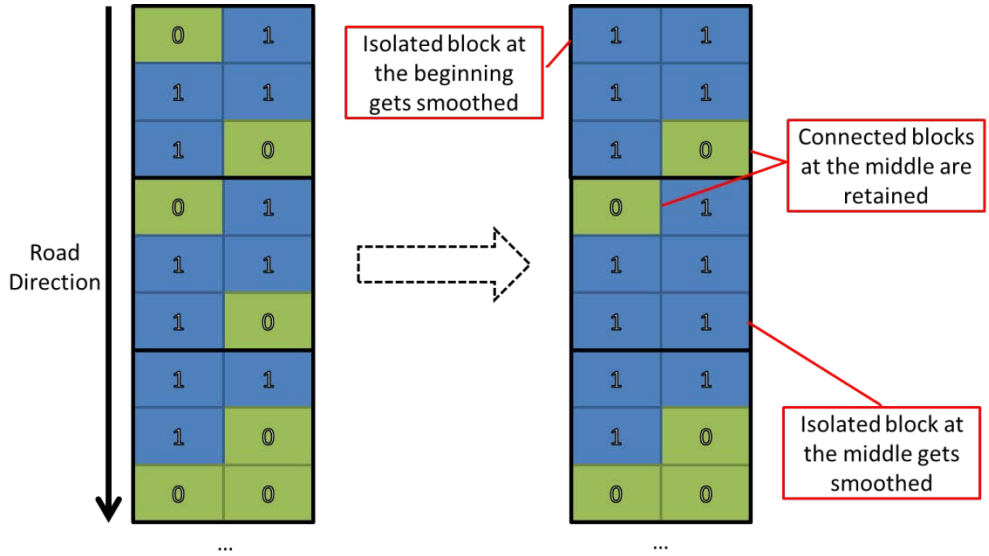

FIGURE 27 Outlier removal example.

After outliers are removed, the next step conducts a smoothness function to retain a continuous, predominant raveling portion by mimicking the actual field survey practice. Based on the field survey practice, it is assumed that the length of pavement with a uniform raveling condition is approximately 200 ft. This interval can be adjusted for other state DOTs. Therefore, a window of approximately 202 ft., with 37 subsections, is used for smoothing. The following describe the major steps:

1) Treat the left wheel path and right wheel path separately. For each subsection in a wheel path, as shown in Figure 28, compute a weighted average on a 2 * 18 + 1 window centered on the subsection (18 subsections backwards, the subsection itself, and 18 subsections forward; therefore, the total length of the window is 202 ft).
2) The weights are defined as a Gaussian distribution along the window with 37 subsections, so the subsections that are further away from the center subsection have less influence in the weighted average. The generated weighted average will be a real number in [0, 3] that is further discretized into 0, 1, 2, or 3. The key parameter here is the variance of Gaussian, which determine how much the nearby subsection influences the raveling level of the center subsection. It is determined by means of a set of comparison experiments that evaluate the performance after applying the Gaussian distribution with different variance values to the raveling classification results.
3) For subsections at boundary (i.e., subsections that are less than 18 positions away from the beginning or the end of the mile), the number of subsections within the side of the windows will be less than the required number of

18. To generate consistent weighted average on boundary subsections, a technique that is commonly used in signal processing is applied here; some subsections are padded over the boundary using mirroring; then the weighted average can be consistently applied over the entire wheel path. Mirroring consists of extending the length of the array by reversing the data.

Repeat the above steps for each subsection. Figure 28 shows an example of subsection smoothness, Figure 29 an example of smoothness.

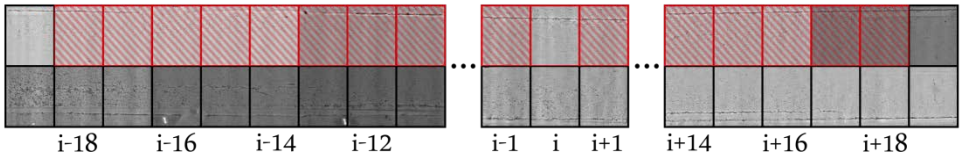

FIGURE 28 Subsection smoothness.

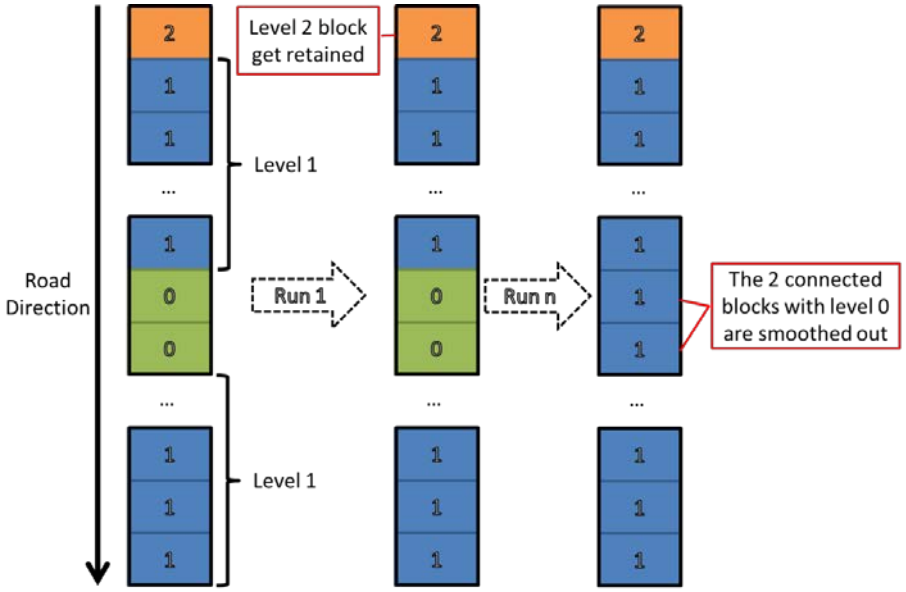

FIGURE 29 Smoothness example.

Finally, within each 1-mile section, the outcomes are aggregated and summed–up; the total percentage of each raveling level is generated.

3.4 TESTING AND VALIDATION OF DEVELOPED ALGORITHMS

The developed algorithms have been tested and validated using the 3D pavement data collected on I-85 and I-285 near Atlanta, Georgia. All the asphalt pavements have open-graded friction course (OGFC). On I-85, four 1-mile test sections were selected. In each test section, a 500-ft sample section was further marked and investigated with a GDOT pavement engineer's assistance. The aggregated test results were compared with GDOT's pavement condition database. On I-285, raveling detection was conducted on the entire highway clockwise and counterclockwise. A GDOT engineer also performed an in-field validation. The following sections present the detailed test results.

3.4.1 Test Sections

3.4.1.1 I-85 Test Sections

Four 1-mile test sections were selected on I-85. In GDOT's pavement condition survey practice, the basic survey unit is about 1 mile. For example, a 10-mile survey project will be divided into ten 1-mile segments. The

pavement condition survey will be conducted on each segment. For raveling, the windshield survey method was used and the total percentage of raveled sections and the predominant severity level were recorded. In our test, four test sections were selected so that each severity level of raveling (including 0; i.e., no raveling) occurs. Figure 30 shows four selected test sections on I-85. The following describe these four test sections:

1) Test Section #1

This test section is located on I-85 South from milepost 87 to 88. The majority of this test section has Severity Level 1 raveling, but some spots show Severity Level 2 and 3 raveling. A 500-ft sampling section was selected for field investigation. A 50-feet-long surface layer loss can be seen clearly from the photos, as shown in Figure 31.

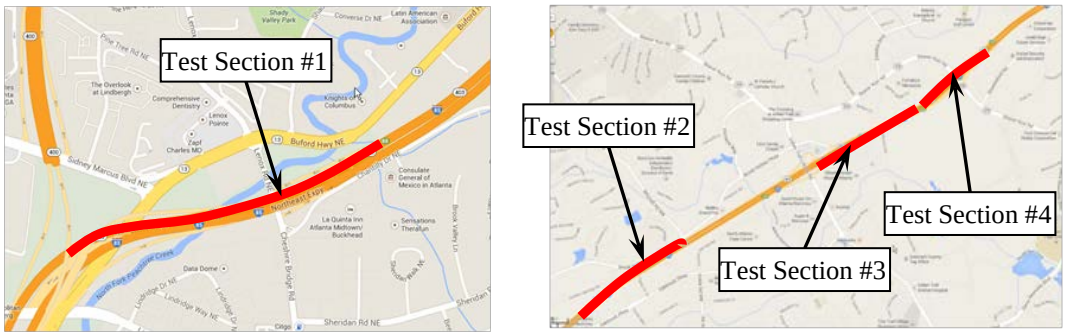

FIGURE 30 Test sections on I-85.

FIGURE 31 Severe raveling on test section #1.

2) Test Section #2

This test section is located on I-85 South from milepost 99 to 100. The majority of this test section shows no raveling. A 500-ft sampling section was selected for field investigation. Figure 32 shows the typical pavement surface.

FIGURE 32 Typical pavement surface on test section #2.

3) Test Section #3

This test section is located on I-85 South from milepost 101 to 102. The majority of this test section shows no raveling. A 500-ft sampling section was selected for field investigation. Figure 33 shows the typical pavement surface.

FIGURE 33 Typical pavement surface on test section #3.

4) Test Section #4

This test section is located on I-85 South from milepost 102 to 103. The majority of this test section shows no raveling. A 500-ft sampling section was selected for field investigation. Figure 34 shows the typical pavement surface.

FIGURE 34 Typical pavement surface on test section #4.

3.4.1.2 I-285 Test Section

I-285 is a major bypass around Atlanta for 18-wheel trucks. As shown in Figure 35, I-285 is about 64 centerline miles. About 47.6% of pavements on I-285 are asphalt concrete (AC) pavements; the other 52.4% are portland cement concrete (PCC) pavements.

To validate the developed raveling detection and classification algorithms, a large-scale test was done on the entire I-285 AC pavement in two directions. The total length is approximately 61 lane-miles. The automatically detected results were validated by a GDOT engineer using a field drive-through.

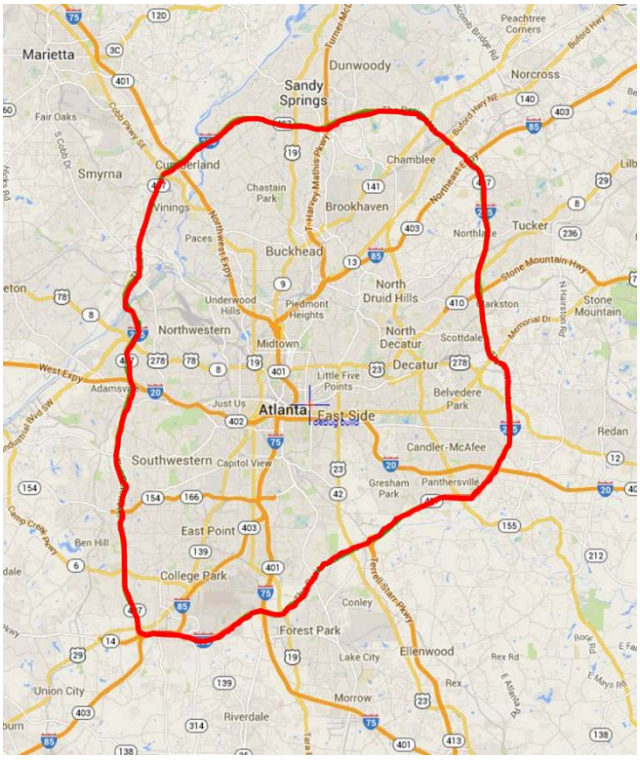

FIGURE 35 I-285 in Atlanta.

3.4.2 Collecting Ground Truth Data Using a Rating Tool

As discussed above, the developed raveling detection and classification algorithms employed a supervised machine learning method that needs to be trained using data with known raveling conditions. This type of data is also known as ground truth. The algorithm has to learn how to recognize raveling Severity Levels 0, 1, 2, and 3 from a large number of ground truth data. Therefore, the correctness and richness of ground truth are very important for the project.

The Georgia Tech research team closely worked with the GDOT engineer to establish the ground truth data. The following major steps were used in the process of establishing ground truth:

1) Data preparation. 3D pavement data collected at some representative sections were used for establishing the ground truth. The sections included four miles of asphalt concrete (AC) pavement on I-85 and 61 miles of asphalt pavement on I-285. Sufficient raveling areas, from Severity Level 0 to Level 3, were covered in the selected sections. For reference, we also collected video log images of the pavement surface using the GTSV.
2) Field raveling survey. After picking the sections, the Georgia Tech research team went to the field with the GDOT engineer (Figure 36). By looking at raveling areas closely, the Georgia Tech research team determined the raveling condition of the selected sections, which was also confirmed by the GDOT engineer.
3) Drive-through evaluation. To validate the automatic raveling detection and classification results, the reference data were collected by the GDOT engineer. Table 5 shows the raveling percentage and the predominant severity level for each test section on I-85.
4) Manual rating. With the knowledge provided by the GDOT engineer, the Georgia Tech research team manually rated the 3D pavement data with different severity levels. The rating process was repeated by several people. This allowed comparison of the manual ratings among different people and identified “difficult” cases (uncertain levels) from “easy” ones (certain levels).

TABLE 5 Raveling Survey on I-85 Test Sections Conducted by GDOT

Test Section #	Percentage (%)	Predominant Severity Level
1	21	1
2	0	0
3	10	1
4	0	0

5) Cross checking. The GDOT engineer helped to double-check the "difficult" cases. By providing both video log (mimicking the input of the manual survey) and 3D pavement data (input of automatic algorithm), the raveling level of most "difficult" cases could be determined.

FIGURE 36 Field raveling investigation on I-85 with GDOT pavement engineer.

To ensure the richness of the ground truth, data from 65 miles (4 miles on I-85 and 61 miles on I-285) of AC pavements to be rated manually, were selected. There were more than 22,000 3D pavement images reviewed. To perform the manual rating process faster and more easily, two rating applications were developed.

1) The first application was used for subsection rating. It displayed the entire 16-ft image (left image in Figure 37) or an individual subsection (right image in Figure 37). It allowed users to choose a severity level and to switch between subsections using keyboard shortcuts.
2) The second one was for image-level rating. It displayed both the 3D pavement data (left image in Figure 38) and the video log image (right image in Figure 38). To simulate the drive-through survey for a manual raveling survey, the application can play the video log images and 3D pavement data at an adjustable speed. When a raveling section was observed, the reviewer pressed a button indicating the raveling level. All the images following are rated as the select level until the raveling section ends or the raveling condition changes.

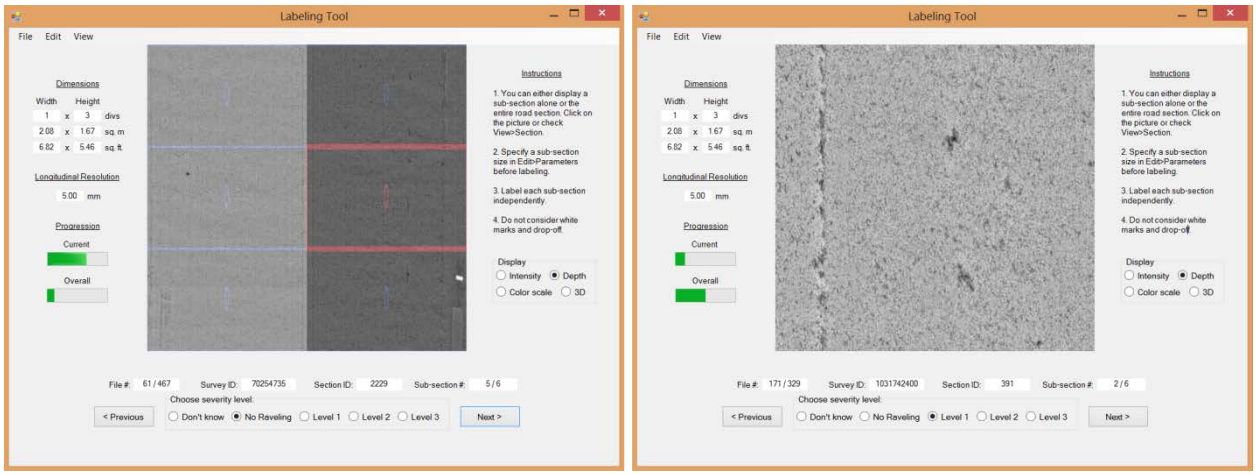

FIGURE 37 Application for subsection-level raveling rating.

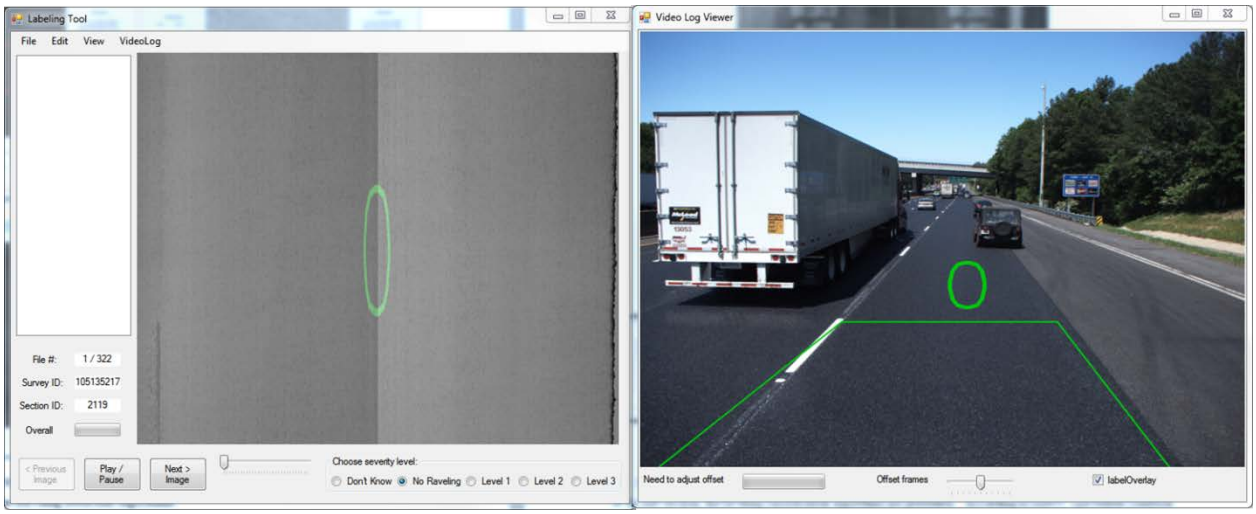

FIGURE 38 Application for image-level raveling rating.

3.4.3 Testing Results on I-85

In highway agency practices, the details at the subsection level are not needed for a raveling condition survey. Normally, raveling is recorded for a certain length of pavement section. In GDOT, the basic unit for a raveling survey is a segment that is normally 1 mile long. More importantly, in a field visual investigation, an engineer often checks a large area for raveling, rather than counting all the small raveled spots.

To mimic the field visual inspection procedures and ensure the raveling condition data were consistent with the past engineering practices, an aggregation algorithm was developed to aggregate all the subsection-level raveling data and report the raveling conditions at segment levels (i.e., 1-mile long pavement section).

3.4.3.1 Comparison Between In-office Rating and In-field Investigation

For validation purposes, manual rating was done for each subsection in the four test sections of I-85. After smoothing using the aggregation algorithm, segment-level ground truth was obtained. This ground truth data were acquired by in-office rating rather than field investigation. Thus, a comparison was needed to assess its accuracy.

As shown in Table 6, although the predominant severity level for each test section was consistent with the field investigation result, the percentage of raveling identified in-office was much less than that acquired in the field. To further validate the results, a forensic study was conducted with the GDOT engineers. After careful review of every single pavement image, GDOT engineers agreed that the in-office result should be more accurate than the in-field

investigation because field investigation was performed by a windshield survey. Because of the difficulties of perceiving pavement texture change accurately from a vehicle traveling at highway speed, the in-office ground truth was adopted.

TABLE 6 Ground Truth Comparison on I-85 Test Sections between In-Office and In-Field Results

Test Section #	Test Method	Percentage (%)	Difference	Predominant Severity Level
1	In-Field	21	10.67	1
	In-Office	31.67		1
2	In-Field	0	0	0
	In-Office	0		0
3	In-Field	10	-9.07	1
	In-Office	0.93		1
4	In-Field	0	0	0
	In-Office	0		0

3.4.3.2 Comparison Between In-Office Ground Truth and Automatic Classification Results

The following will compare the aggregated raveling data for each test section based on the automatic detection and classification results with the ground truth acquired from in-office rating.

1) Test Section #1

Table 7 shows the validation results for Test Section #1. Based on GDOT's protocol, the predominant severity level is 1, and the total raveling percentage is 32.6% (31.67% + 0.93% + 0%). The automatic classification results show total 37.88%. There is a difference of 6.21%. In considering the subjective factor in the manual rating, this difference should not be significant.

TABLE 7 Segment-level Comparison for Test Section #1

	Level 0 (%)	Level 1 (%)	Level 2 (%)	Level 3 (%)	Predominant
Ground Truth	67.4	31.67	0.93	0	1
Automatic Results	62.12	37.88	0	0	1
Absolute Error	5.28	6.21	0.93	0	—

Figure 39 compares the distribution of raveling between the ground truth and the automatic results, which were aggregated every 0.01 mile. It can be seen that the distribution of the automatic detected and classified raveling is close to that from the ground truth data.

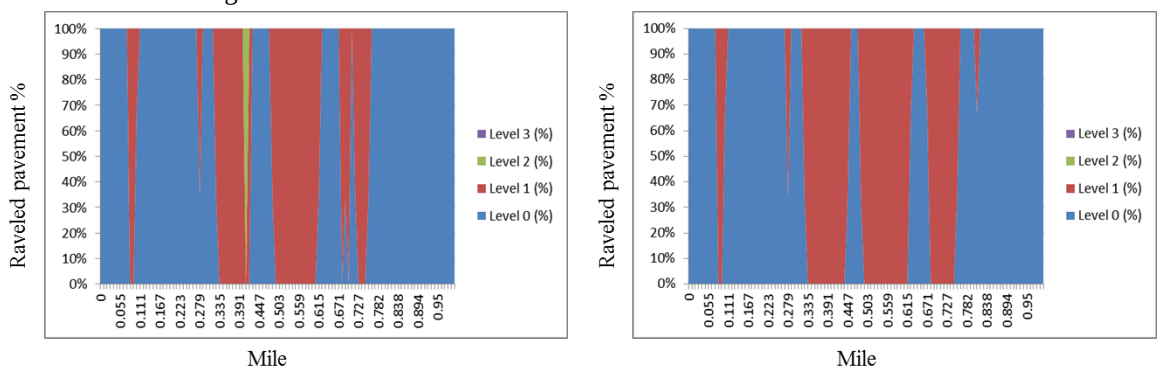

(a) Ground Truth **(b) Automatic Results**

FIGURE 39 Raveling distribution in test section #1.

2) Test Section #2

Table 8 shows the validation results for Test Section #2. It can be seen that the automatic results exactly match the ground truth, in which no raveling appears.

TABLE 8 Segment-level Comparison for Test Section #2

	Level 0 (%)	Level 1 (%)	Level 2 (%)	Level 3 (%)	Predominant
Ground Truth	100	0	0	0	0
Automatic Results	100	0	0	0	0
Absolute Error	0	0	0	0	—

Figure 40 compares the distribution of raveling between the ground truth and the automatic results, which were aggregated every 0.01 mile. It can be seen that the distribution of the automatic detected and classified raveling is exactly same with that from the ground truth data.

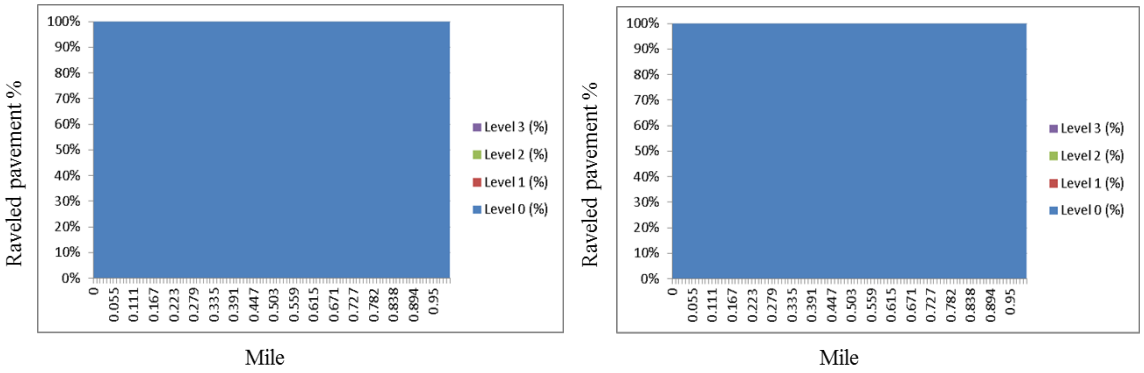

(a) Ground Truth **(b) Automatic Results**

FIGURE 40 Raveling distribution in test section #2.

3) Test Section #3

Table 9 shows the validation results for Test Section #3. Based on GDOT's protocol, the predominant severity level is 1; however, the raveling extent is very small, 0.93%, which is essentially 0. The automatic results show no raveling. In GDOT's pavement condition survey protocol, the required accuracy for raveling extent is 5%. Thus, the difference for Test Section #3 can be ignored. It can be considered that the automatic results coincide with the ground truth.

TABLE 9 Segment-level Comparison for Test Section #3

	Level 0 (%)	Level 1 (%)	Level 2 (%)	Level 3 (%)	Predominant
Ground Truth	99.06	0.93	0	0	1
Automatic Results	100	0	0	0	0
Absolute Error	0.93	0.93	0	0	—

Figure 41 compares the distribution of raveling between the ground truth and the automatic results, which were aggregated every 0.01 mile. It can be seen that the automatic detected and classified results underestimated the raveling at mile 0.503 and 0.615. However, the value is small.

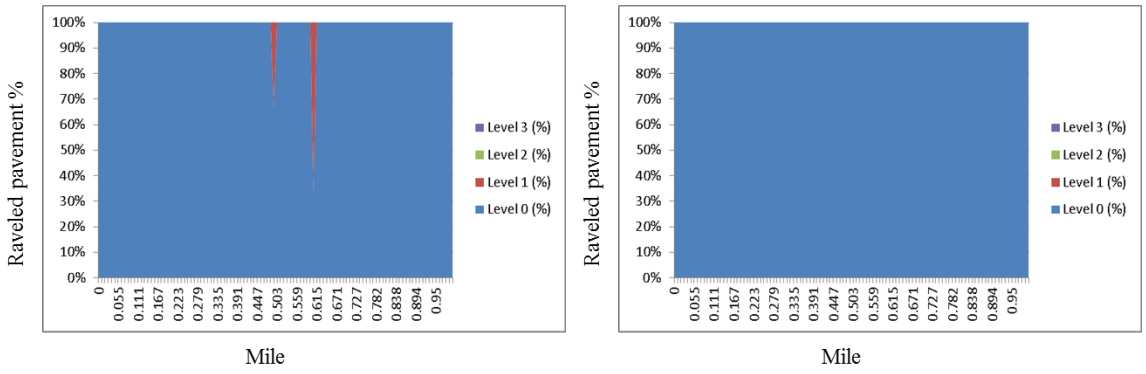

(a) Ground Truth **(b) Automatic Results**

FIGURE 41 Raveling distribution in test section #3.

4) Test Section #4

Table 10 shows the validation results for Test Section #4. The ground truth shows no raveling in this section. However, the automatic results show 0.31% of Severity Level 1 raveling. Since the number is very small, the automatic results and the ground truth are, essentially, the same.

TABLE 10 Segment-level Comparison for Test Section #4

	Level 0 (%)	Level 1 (%)	Level 2 (%)	Level 3 (%)	Predominant
Ground Truth	100	0	0	0	0
Automatic Results	99.68	0.31	0	0	1
Absolute Error	0.31	0.31	0	0	—

Figure 42 compares the distribution of raveling between the ground truth and the automatic results. The automatically detected and classified results are very close to the ground truth.

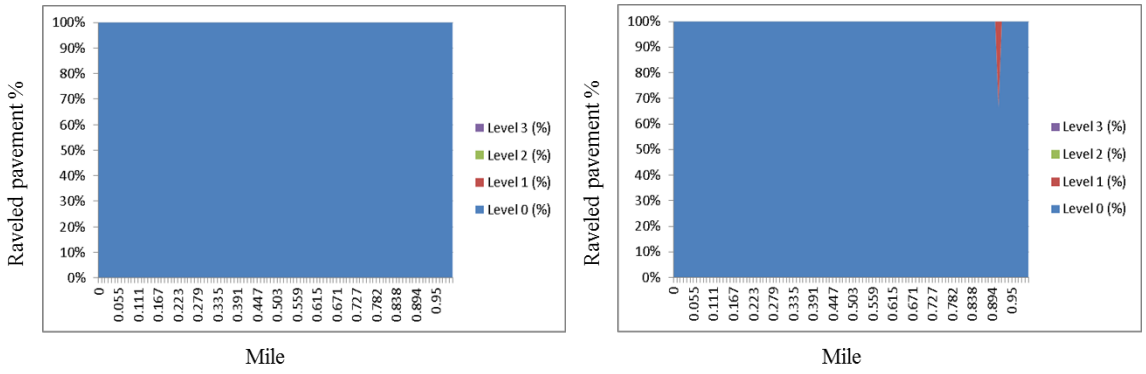

(a) Ground Truth (b) Automatic Results

FIGURE 42 Raveling distribution in test section #4.

3.4.4 Testing Results on I-285

Similarly, automatic raveling detection and classification were performed on I-285. The following compares the aggregated raveling data for each test section with the ground truth acquired from in-office rating. For better visualization, only the comparison results of the south half of I-285 pavement are shown, which shows raveling. The north half are neglected since the pavement is either concrete or newly resurfaced asphalt. In general, all

segments without raveling were 100% detected and classified. The predominant raveling severity level of all raveled segments was also 100% classified (which is severity level 1).

Figure 43 and Figure 44 compare the extents (i.e., percentage) of portions with no raveling or predominant raveling level (Severity Level 1) in each segment. The reference is obtained by manually rating the raveling levels on the complete I-285 loop (clockwise and counterclockwise). In most sections, the difference in the percentage of predominant raveling between aggregation results and ground truth is around 10%. However, there are some cases in which the differences are larger than 15%, which may be due to several reasons:

1) Ground truth rating: As mentioned before, there are several "difficult" cases for manual rating. Although they are assigned ratings, the consistency between these cases is hard to ensure. There are two challenges: (1) definition of Severity Level 1 or in the border; and (2) the measurement of a mixed raveling condition, including no raveling.
2) Noise in 3D data: Other surface distresses, such as scratches and cracking, have strong effects on the raveling classification algorithm. Although some noise removal modules have been developed and applied, it is still not possible to remove all the noise from the testing data at current stage.
3) In some sections, the sum of no-raveling percentage and predominant raveling percentage is much less than 100%. Those cases are due to the existence of concrete pavements in the section, which were contributing to the denominator of the percentage. A precise pavement type classification algorithm will be helpful in solving the issue in the future. At this moment, we can still evaluate the performance of raveling detection and classification by checking the relative difference between ground truth percentage and algorithm percentage.

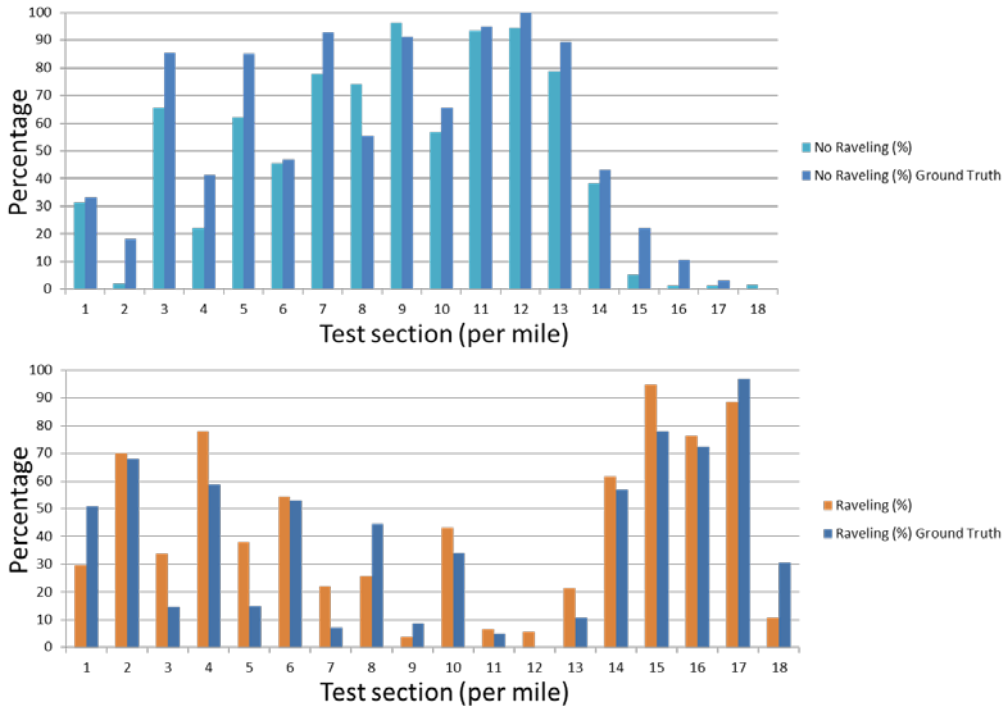

FIGURE 43 Segment-level comparison for I-285 clockwise test sites.

To get a better idea of the raveling aggregation results, the aggregation results of I-285 test sections on a map (Figures 45 and 46) were overlaid. On the left part of the figure, a map is displayed with raveling aggregation results. Sections with red lines are classified as raveling sections (Level 1 in this case). Green sections are considered as no-raveling. On the right part of the figure, a histogram showing the raveling percentage along driving direction of I-285 is given. According to a previous field survey, the southbound lane of I-285 has severe Level 1 raveling. Similar observations can be found in both the map-representation and the histogram-representation.

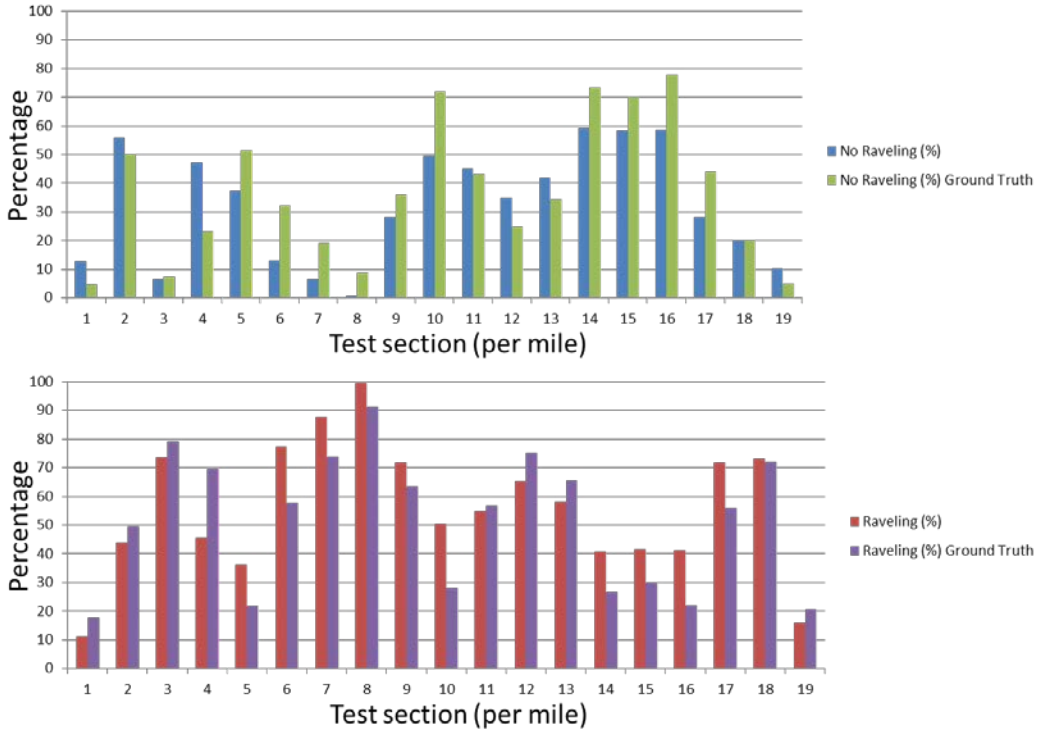

FIGURE 44 Segment-level comparison for I-285 counter clockwise test sites.

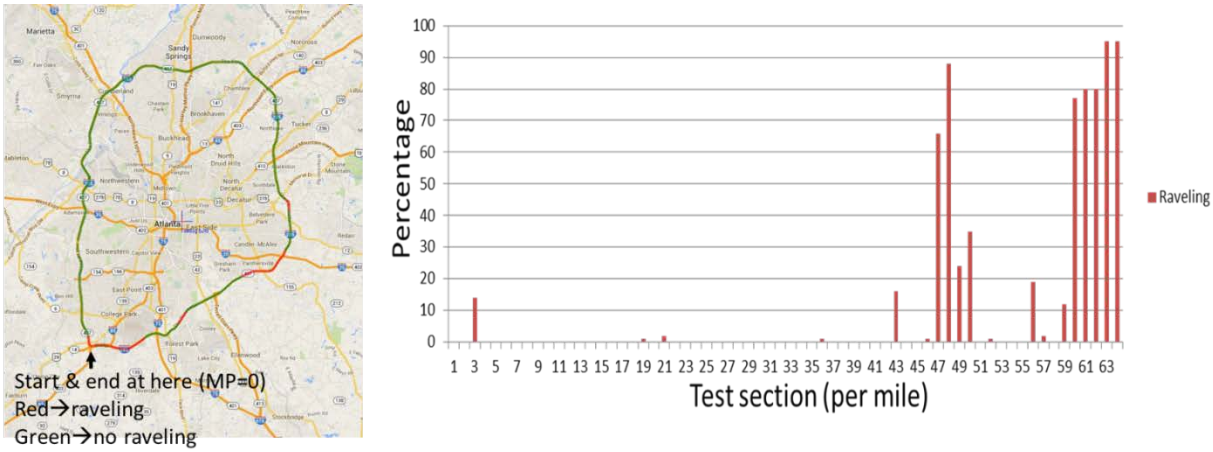

FIGURE 45 Percentage of predominant raveling (Level 1) along I-285 clockwise testing sites.

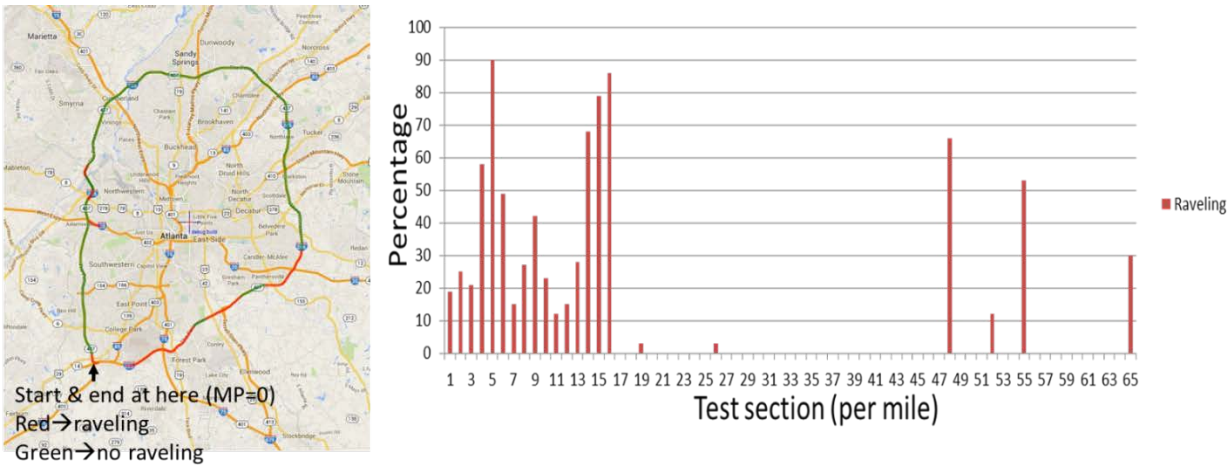

FIGURE 46 Percentage of predominant raveling (Level 1) along I-285 counterclockwise testing site.

To further check the correctness of the raveling classification results, a visualization tool is proposed for reviewers to investigate the data at different scales. The idea is shown in Figures 47 and 48. On the left, an overview of the aggregation results is provided. In the middle, a zoom-in view of a 1-mile test section is displayed. At the right, a video-log image of a specific 5-m section is given for in-detail validation. Such a tool can be very helpful for both results validation and visualization.

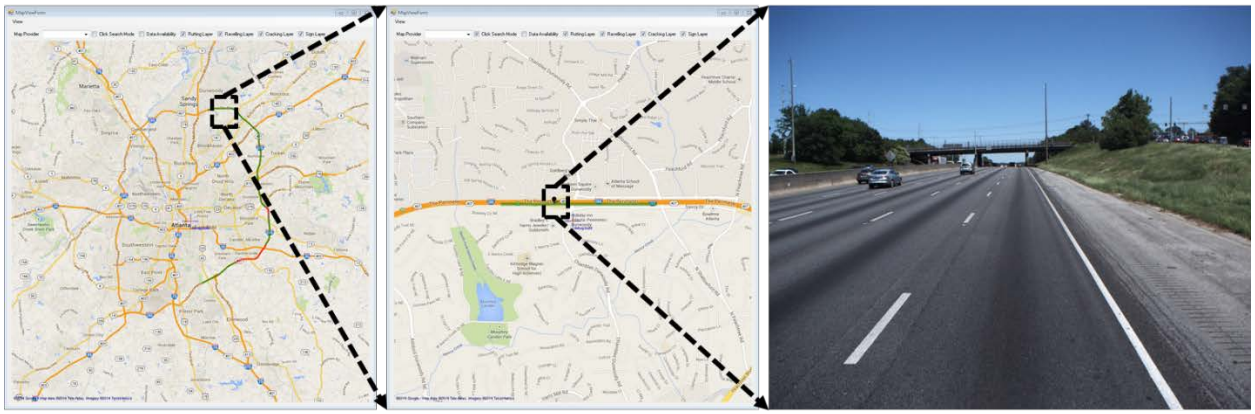

FIGURE 47 Visualization example of no-raveling spot.

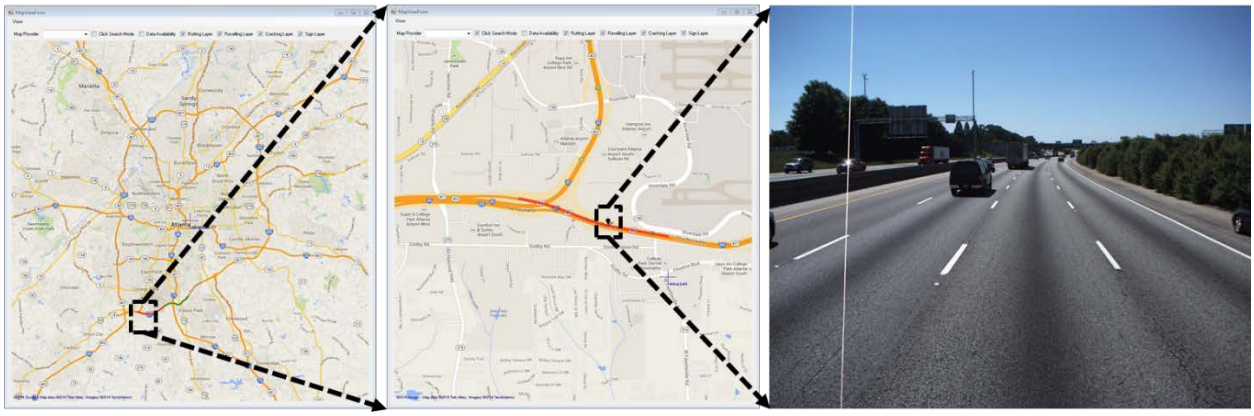

FIGURE 48 Visualization example of raveling spot.

4 PLANS FOR IMPLEMENTATION

With the support of the IDEA concept exploration research project, a set of algorithms has been developed to automatically detect and classify asphalt pavement raveling using 3D pavement data. The preliminary tests demonstrate that these developed algorithms are promising and provide new capabilities to significantly reduce the cost and time spent by state DOTs for visual asphalt pavement raveling surveys.

The IDEA concept exploration research outcomes, including the developed algorithms and applications, could be migrated to national demonstration for a large-scale implementation in the future. The research will, also, allow the developed algorithms tested under real-world environmental conditions in which different raveling protocols in different highway agencies and different surface materials can be adapted.

Based on the developed algorithms, software will be developed to effectively perform raveling detection and classification. GIS technology can also be incorporated into the pavement raveling survey and management system.

5 CONCLUSIONS AND RECOMMENDATIONS

As one of the most common asphalt pavement distresses, raveling increases pavement roughness, which results in poor ride quality, road and tire noise, and safety issues. Besides safety concerns, including loose stones that may break windshield glass and potential hydroplaning, raveling shortens pavement longevity. Thus, a raveling condition survey is critically needed so highway agencies know where and how severe their raveling is. Then, appropriate preservation or rehabilitation treatments can be applied. To address the above urgent need, the Georgia Tech research team developed new raveling detection and classification algorithms using 3D pavement data with artificial intelligence and machine learning.

The raveling detection and classification algorithms presented in this final report were the first to be comprehensively validated using large-scale 3D pavement data with real-world transportation agencies' raveling survey protocol (e.g., severity levels 1, 2, and 3 of GDOT). Although it was tested and validated using GDOT's pavement condition survey protocol, the proposed framework, including the algorithms and procedures could be extended to other transportation agencies with some modification. If a different raveling classification protocol is used, the proposed raveling classification algorithms could be re-trained using a set of ground truth data classified by the targeted raveling classification protocol. The framework, algorithms, and process are the same, although the testing and validation are still needed for different raveling protocols.

The algorithms were comprehensively tested and validated on I-85 and I-285 near Atlanta, Georgia. The following summarizes the research outcomes and major findings:

1) Using 3D pavement data and the accompanying 2D intensity data, the proposed raveling detection and classification algorithms consist of five major components:
    a) data pre-processing,
    b) pavement texture feature computation,
    c) subsection-level raveling classification,
    d) post-processing for section raveling data smoothing from subsection-level raveling classification, and
    e) aggregation of the detection outcomes to segment-level measurement of raveling.
2) To validate the proposed algorithms, four test sections were selected on I-85, and the entire AC pavements were selected on I-285 in Atlanta, Georgia. A total of 65 miles (4 miles on I-85 and 61 miles on I-285) of pavement sections were selected to establish the ground truth. Working with GDOT engineers, ground truth data were established through in-field survey and in-office review of videolog image and 3D pavement data.
3) The following are the comprehensive testing results of four test sections on I-85:
    a) In GDOT's raveling survey protocol, only the predominant severity level and the total raveled percentage is recorded. Given the fact that Severity Level 1 is the most predominant one in most cases on interstate highways, the currently trained algorithms are very accurate for GDOT's use, since the lump sum of all types of raveling is very accurate.
    b) A comparison was performed between the in-field survey and the in-office manual rating. The results showed the difference. Working with GDOT engineers, the Georgia Tech research team carefully reviewed the entire 3D pavement data and the video log images. The in-office results are considered to be more accurate because the perception of pavement surface texture change by a person sitting in a vehicle at highway speed can be very different. Thus, the in-office manual rating results were considered as the ground truth.
    c) After aggregating the classified subsection results, the automatic classification results on each test section were compared with the ground truth. The difference of total raveled percentage on Test Section #1 is about 6.21%, and is less than 1% for the other three test sections. The predominant severity levels (Severity Levels 1, 2, or 3) for Test Sections #1 and #2 are also correctly classified.

For Test Sections #3 and #4 there is essentially no raveling, and the classification errors are 0.93% and 0.31%.

4) The testing on 61 lane-miles of I-285 AC pavements shows promising results for automatic raveling detection and classification. All the pavements with or without raveling were 100% correctly detected and classified at the segment level; each segment is 1mile long. However, due to the difficulty of correctly rating all the raveling areas using video log images and 3D pavement data and due to the impact of cracking and flat-tire scratches, the raveling extent (percentage) shows a certain level of variation in comparison with the manually labeled ground truth. The difference between the surveyed results that were conducted by the experienced GDOT engineer and the automatically detected and measured results is less than 15%, and most of them are less than 10%.

In summary, the proposed algorithms have demonstrated the promising capabilities of automatically detecting, classifying, and measuring asphalt pavement raveling. This will potentially save tremendous amounts of manual effort for field surveys, improve the data accuracy, and help highway agencies make more informed decisions on pavement maintenance and rehabilitation.

The following are recommendations for future research:

1) More testing and validation are suggested to evaluate the performance of the developed algorithms on pavements of different raveling conditions, ages, and surface types [e.g., dense grade asphalt pavement, stone matrix asphalt (SMA) pavement, etc.].
2) Further refinement is suggested to reduce the impact of other distresses, such as cracking and flat-tire scratches, on raveling detection and classification. It will require the detection of those unrelated distresses and performance of a removal process.
3) Beyond GDOT's pavement condition survey protocol for raveling, a more detailed indicator developed for raveling; for example, percentage of aggregate loss, is recommended. The current raveling classification method (Severity Levels 1, 2, and 3) is somewhat coarse for depicting the loss of aggregate on asphalt pavements, which might not be sufficient to indicate the best timing for a preventive maintenance method; for example, fog seal. Thus, a finer indicator is desirable.

REFERENCES

Benyamin, D. (Nov. 10, 2012). *A Gentle Introduction to Random Forests, Ensembles, and Performance Metrics in a Commercial System* [Online]. Available: http://citizennet.com/blog/2012/11/10/random-forests-ensembles-and-performance-metrics/ [accessed July 2014].

Breiman, L. (Oct. 2001). "Random Forests," *Machine Learning*, Vol. 45, No. 1, pp. 5–32.

Cortes, C. and V. Vapnit (1995). *Support-Vector Networks*, *Machine Learning*, Vol. 20, pp. 273–297.

Cutler, D.R., T.C. Edwards, Jr., K.H. Beard, A. Cutler, K.T. Hess, J. Gibson, and J.J. Lawler (2007). "Random Forests for Classification in Ecology," *Ecology*, Vol. 88, No. 11, pp. 2783–2792.

FDOT (2015). *Flexible Pavement Condition Survey Handbook*, Florida Department of Transportation, Tallahassee.

FHWA (2014). *Distress Identification Nanual for the Long-Term Pavement Performance Project*, FHWA-RD-03-031, Federal Highway Administration, Washington, D.C.

GDOT (2007). *Pavement Condition Survey Manual*, Georgia Department of Transportation, Atlanta.

Jiang, C. and Y. Tsai (2015) *Enhanced Crack Segmentation Algorithm Using 3D Pavement Data*, ASCE, *Journal of Computing in Civil Engineering*, in press.

Laurent, J., J.F. Hebert, D. Lefebvre, and Y. Savard (2012a). *Using 3D Laser Profiling Sensors for the Automated Measurement of Road Surface Conditions*, 7th RILEM International Conference on Cracking in Pavements, Delft, the Netherlands, June 20–22, 2012.

Laurent, J., J.F. Hebert, D. Lefebvre, and Y. Savard (2012b). *High-Speed Network Level Road Texture Evaluation Using 1mm Resolution Transverse 3D Profiling Sensors Using A Digital Sand Patch Model*, 7th International Conference on Maintenance and Rehabilitation of Pavements and Technological Control, Auckland, New Zealand, Aug. 28–30, 2012.

Mathavan, S., M. Rahman, M. Stonecliffe-Jones, and K. Kamal (2014). "Pavement Raveling Detection and Measurement from Synchronized Intensity and Range Images," *Transportation Research Record: Journal of the Transportation Research Board, No. 2457*, Transportation Research Board of the National Academies, Washington, D.C., pp. 3–11.

McRobbie, S. and G. Furness (2008). *Automated Detection of Fretting on HRA Surfaces*, TRL Published Project Report 229, Transport Research Laboratory, Wokingham, Berks, U.K., 16 pp.

McRobbie, S., J. Iaquinta, A. Wright, P. Trumper, and J. Kennedy (2012). *Development and Validation of Algorithms for the Automatic Detection of Fretting Based on Multiple Line Texture Data*, Research into Pavement Surface Disintegration. Phase 2 Interim Report, Transport Research Laboratory, Wokingham, Berks, U.K.

McRobbie, S., C. Wallbank, K. Nesnas, and A. Wright (2015). *Use of High-Resolution 3-D Surface Data to Monitor Change over Time on Pavement Surfaces*, Research into Pavement Surface Disintegration. Phase 3, Transport Research Laboratory, Wokingham, Berks, U.K..

MnDOT (2000). *Best Practices Handbook on Asphalt Pavement Maintenance*, Minnesota T2/LTAP Program, St. Paul.

Miradi, M. (2004). *Neural Network Models for Analysis and Prediction of Raveling*, Proceedings of the 2004 IEEE Conference on Cybernetics and Intelligent Systems (CIS).

NDOR (2002). *Pavement Maintenance Manual*, Nebraska Department of Roads, Omaha.

NYSDOT (2000). *Comprehensive Pavement Design Manual*, New York State Department of Transportation, Albany.

ODOT (2010). *Pavement Distress Survey Manual*, Oregon Department of Transportation, Salem.

Ooijen, V.W. and V.D. Bol (2004). *High-Speed Measurement of Raveling on Porous Asphalt. Symposium on Pavement Surface Characteristics of Roads and Airports*, Toronto, ON, Canada.

Scott, P., K. Radband, M. Zohrabi, P. Sanders, S. McRobbie, and A. Wright (June 2008). *Measuring Surface Disintegration* (*Raveling or Fretting*) *Using Traffic Speed Condition Surveys*, 7th International Conference on Managing Pavement Assets, Calgary, AB, Canada, June 23–28, 2008..

Tsai, Y. and F. Li (2012). *Detecting Asphalt Pavement Cracks under Different Lighting and Low Intensity Contrast Conditions Using Emerging 3D Laser Technology*, *Journal of Transportation Engineering*, ASCE, Vol. 138, No. 5, pp. 649–656.

Tsai, Y., Y. Wu, C. Ai, and E. Pitts (2012). *Feasibility Study of Measuring Concrete Joint Faulting Using 3D Continuous Pavement Profile Data*, *Journal of Transportation Engineering*, ASCE, Vol. 138, No. 11, pp. 1291–1296.

Tsai, Y.C. and Z. Wang (2013). *A Remote Sensing and GIS-Enabled Asset Management System* (*RS-GAMS*). Final Report for USDOT project: DTOS59-10-H-0003, Georgia Institute of Technology, Atlanta.

Tsai, Y., Y. Wu, and Z. Lewis (2014). *Full-Lane Coverage Micromilling Pavement-Surface Quality Control Using Emerging 3D Line Laser Imaging Technology*, *Journal of Transportation Engineering*, ASCE, Vol. 14, No. 2.

Tsai, Y., Z. Wang, and F. Li (2015) "Assessment of Rut Depth Measurement Accuracy of Point-based Rut Bar Systems Using Emerging 3D Line Laser Imaging Technology," *Journal of Marine Science and Technology*, Vol. 23, No. 3, 2015, pp. 322–330.

Tsai, Y. and Z. Wang (2015) *Technology Overview on Validating 3D Transverse Profile Data and Measurement of Pavement Surface Distresses*, Federal Highway Administration, Washington, D.C., June 2, 2015.

TxDOT (2009). *Pavement Management Information System: Rater's Manual*, Texas Department of Transportation, Austin.

WSDOT (1999). *Pavement Surface Condition Field Rating Manual for Asphalt Pavements*, Northwest Pavement.